Gaia

Stereoscopic Census of our Galaxy

https://www.cosmos.esa.int/web/gaia/home https://gaia.ac.uk

one billion pixels for one billion stars

one percent of the visible Milky Way

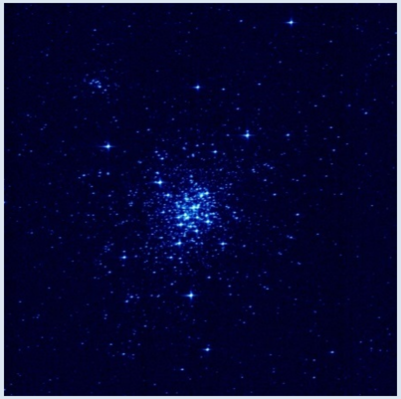

Gerry Gilmore FRS, UK Gaia PI

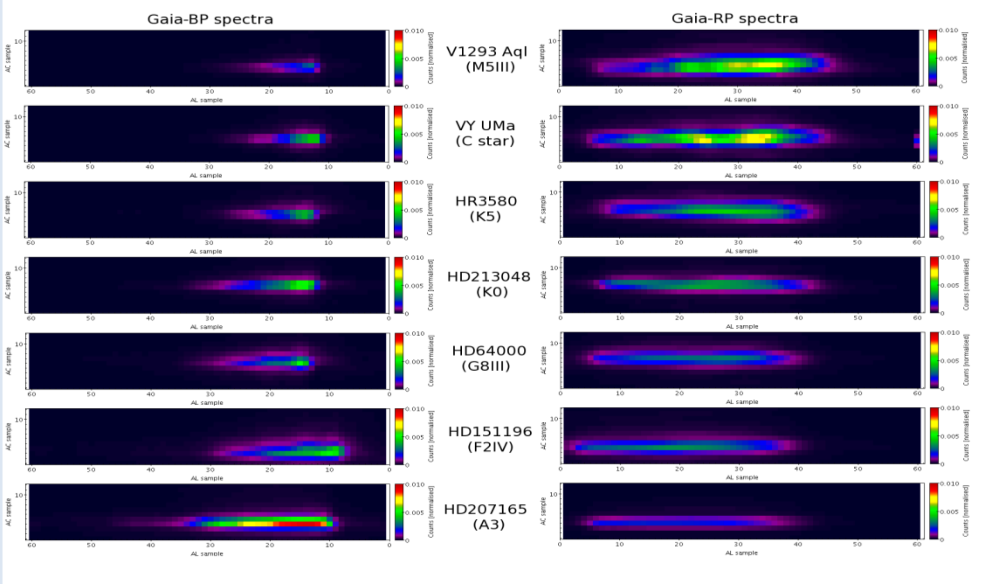

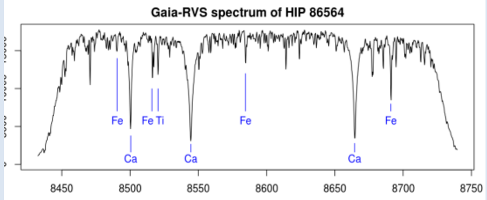

Astrometry, photometry, spectroscopy, spectrophotometry

École Internationale Daniel Chalonge

SCIENCE **WITH GREAT** INTELLECTUAL **ENDEAVOUR AND A** HUMAN **FACE**
SCIENCE AVEC UNE TRES GRANDE EXIGENCE **INTELLECTUELLE** ET UN VISAGE **HUMAIN**

Daniel Chalonge Medal
coined by the "Monnaie de Paris"

TRIBUTE TO HÉCTOR J.DE VEGA

THE SCIENTIST AND THE HUMAN PERSON

http://chalonge.obspm.fr/Cias_Meudon2015.html
http://chalonge.obspm.fr/colloque2015.html
http://chalonge.obspm.fr/Programme2015.html

http://chalonge.obspm.fr

Réalisation : J. Berthier, E. Vergnaud

This talk

- Introduce Gaia
- State of the data processing
- A few science examples/the future
- Gaia and Dark Matter
- Gaia and the evolution of the Milky Way
- Gaia and gravitational waves

The scientific revolution: look at Nature, not authority

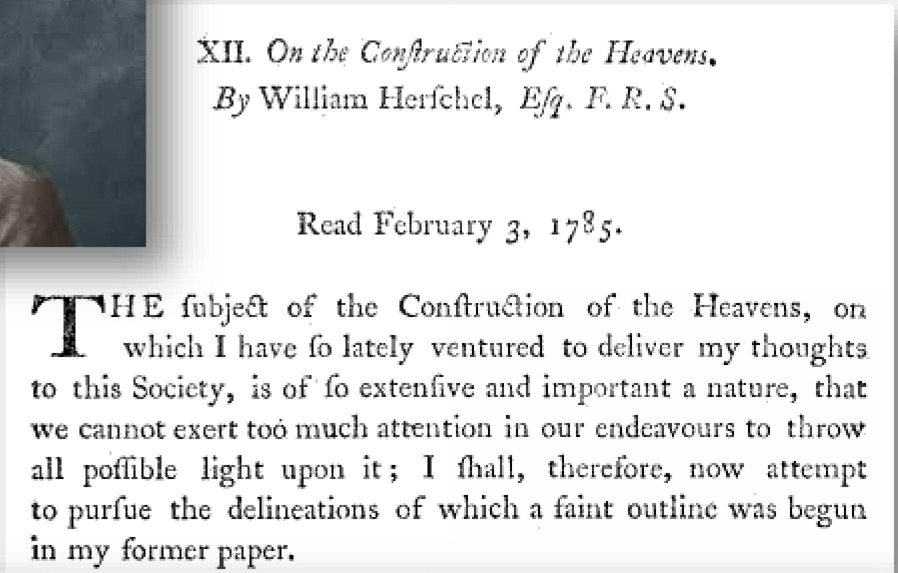

XII. *On the Conſtruction of the Heavens.* *By* William Herſchel, *Eſq. F. R. S.*

Read February 3, 1785.

THE ſubject of the Conſtruction of the Heavens, on which I have ſo lately ventured to deliver my thoughts to this Society, is of ſo extenſive and important a nature, that we cannot exert too much attention in our endeavours to throw all poſſible light upon it; I ſhall, therefore, now attempt to purſue the delineations of which a faint outline was begun in my former paper.

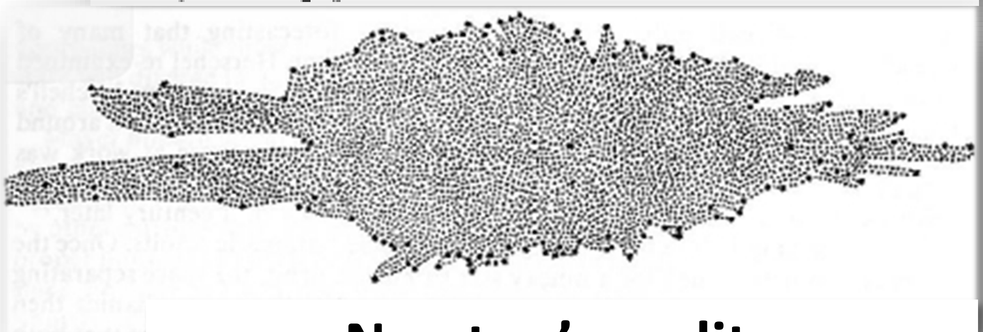

Newton's reality

He could not imagine ideas beyond his "simulation"

Gaia: the goddess who created the universe and knowledge

Gaia is transformational – the first 3-D galaxy
precision distances and motions for 1 billion stars

- Astrometry, photometry, spectroscopy, spectrophotometry, Teff, log g, Av, [Fe/H], binarity, planets, periods for variables,…

Launch: 12/2013

Work started: ~1993
Project approved: 2000
Operations start 7/2014
10 years data
Project end: 2030

Total cost: 960M€

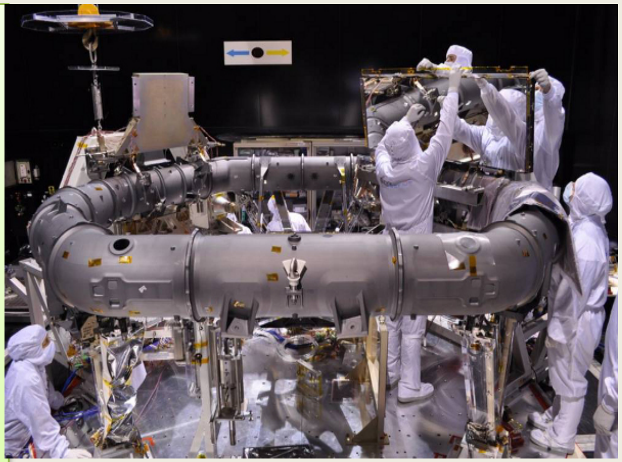

The heart of Gaia is a large camera array, 1 giga-pixel, sending us a video of the sky for 10 years.

The imaging data is being processed in Cambridge.
1.6trillion images processed now

2 telescopes, 1.45 x 0.5 m primary, monolithic SiC optical bench, 0.06arcsec pixels

https://www.cosmos.esa.int/web/gaia/home


The IoA Gaia team
+ Edinburgh, Leicester, MSSL, RAL, Italy, Spain
gaia mapping the milky way from space

Gaia’s Milky Way

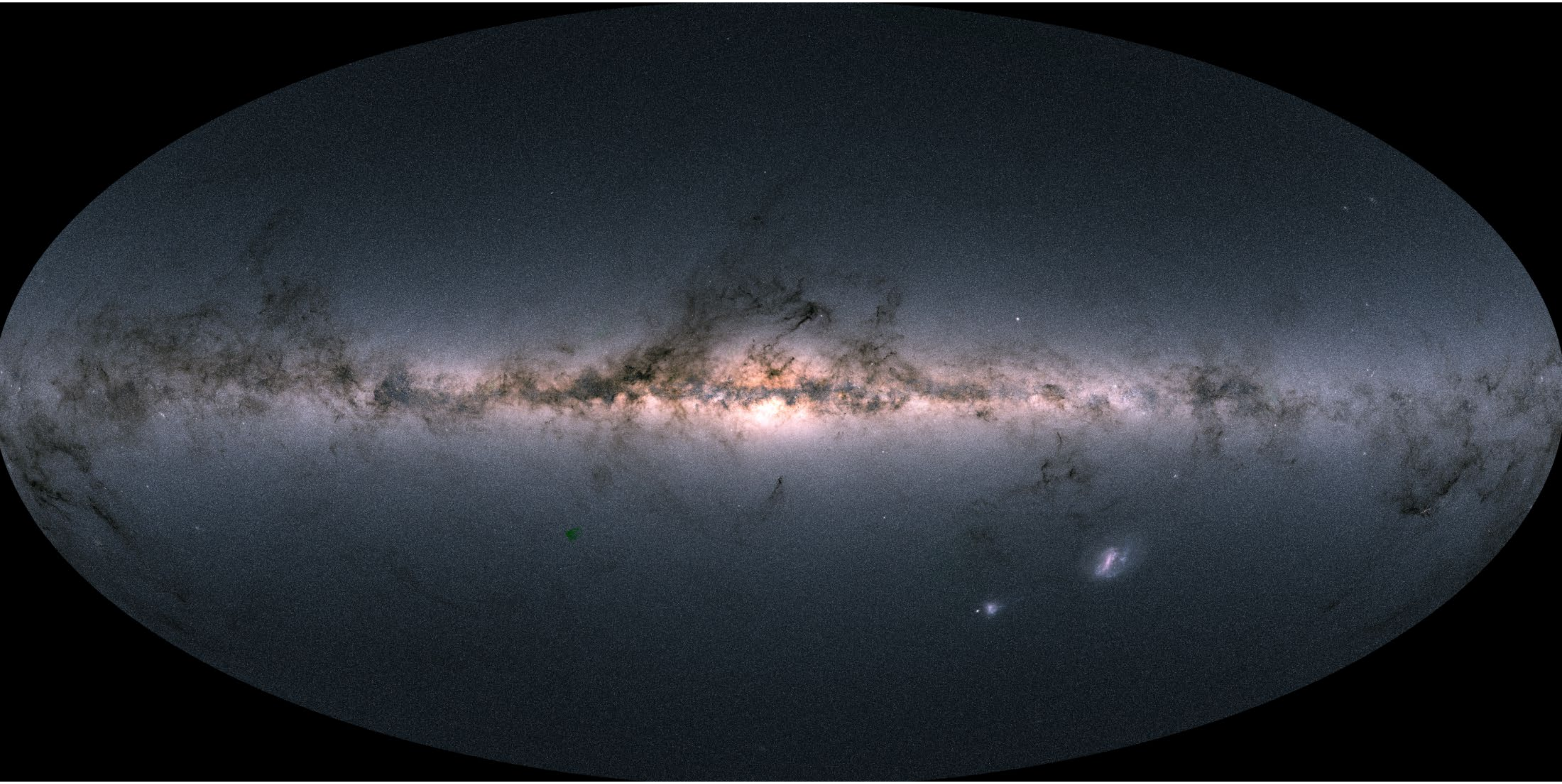

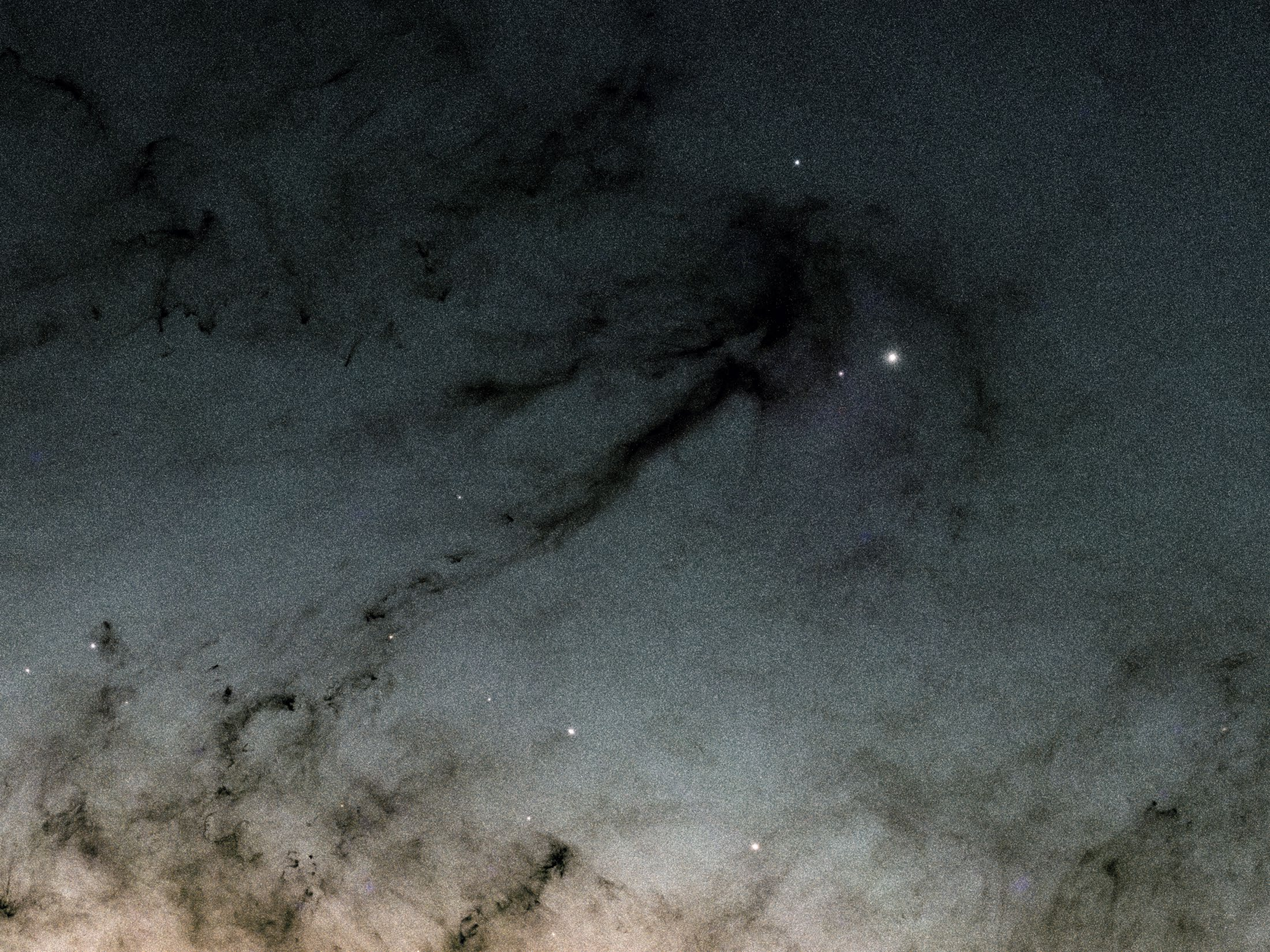

GAIA: Key Science Objectives

⇒ Origin, Formation and Evolution of the Galaxy

Structure and kinematics of our Galaxy:

- shape and rotation of bulge, disk and halo
- internal motions of star forming regions, clusters, etc
- nature of spiral arms and the stellar warp
- space motions of all Galactic satellite systems

Stellar populations:

- physical characteristics of all Galactic components
- initial mass function, binaries, chemical evolution
- star formation histories

Tests of galaxy formation:

- dynamical determination of dark matter distribution
- reconstruction of merger and accretion history

- data support revolutionary science from solar system to cosmology, planets, fundamental physics…

Quantify the history of the growth of structure, chemical and dynamical evolution in our local Universe.

•in our Galaxy …

–the distance and velocity distributions of all stellar populations
–the spatial and dynamic structure of the disk and halo
–its formation history
–a detailed mapping of the Galactic dark-matter distribution
–a rigorous framework for stellar-structure and evolution theories
–a large-scale survey of extra-solar planets (~70,000 systems)
–a large-scale survey of Solar-system bodies (~250,000)

•… and beyond

–definitive distance standards out to the LMC/SMC
–rapid reaction alerts for supernovae and burst sources (~10,000)
–quasar detection, redshifts, lensing structures (1,000,000)
–fundamental quantities to unprecedented accuracy: e.g. relativistic light bending due to gravity: PPN $\sigma_\gamma \sim 2\times10^{-6}$ (~2×10^{-5} present)

$$\sigma_\gamma \approx 1\times10^{-6} \text{ to } 3\times10^{-7}$$

ESA maintains a (conservative) publication list per-mission, based on significant data use
While not a simple ADS search, it is consistent across missions. HST data from STScI.

Since DR2, Gaia has done very well.

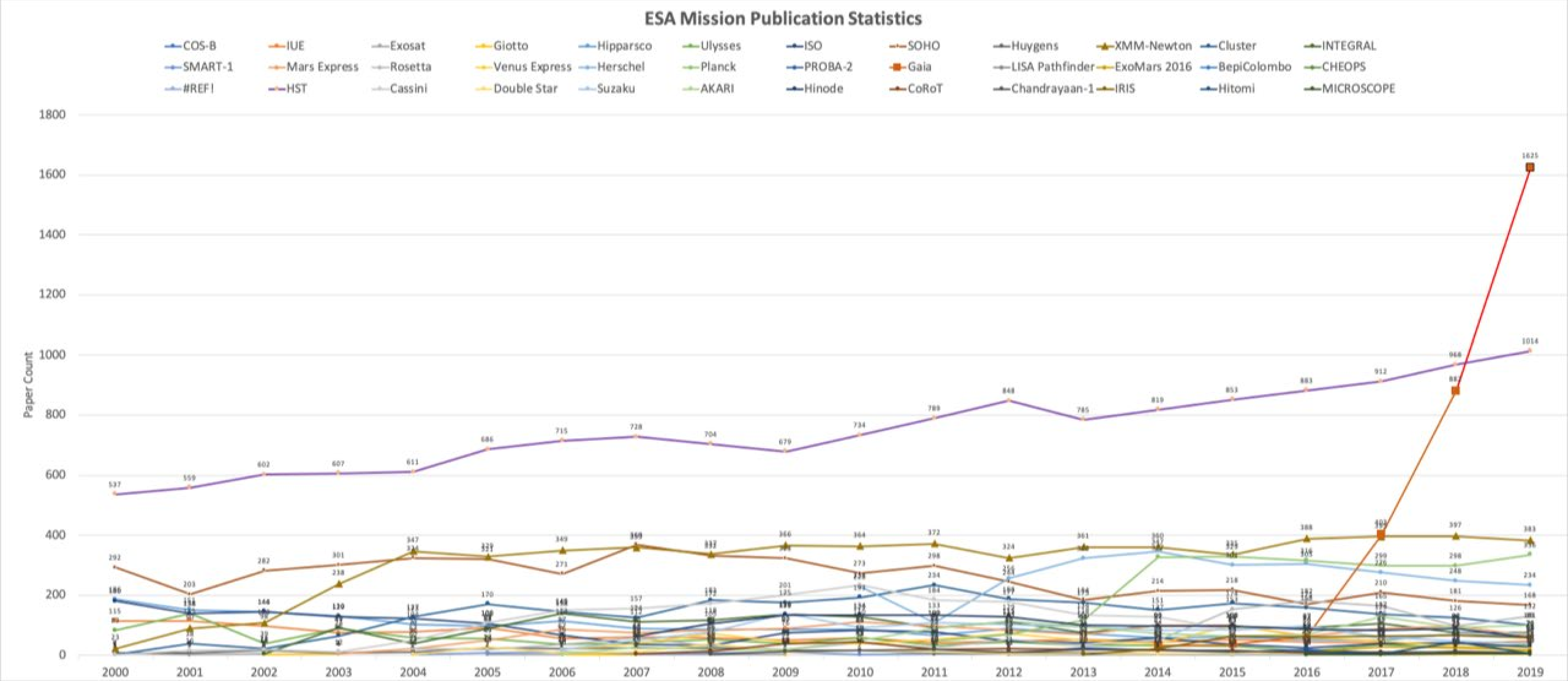

How does Gaia work?: Sky Scanning Principle

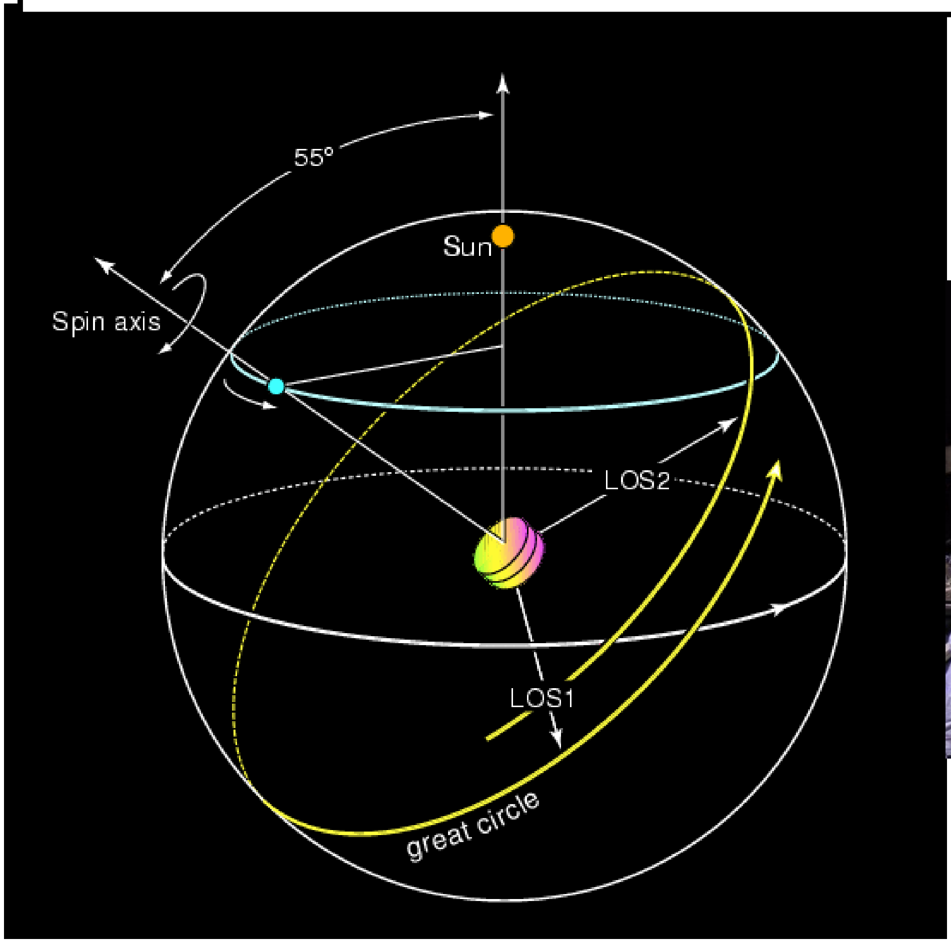

Observe sky with two telescopes

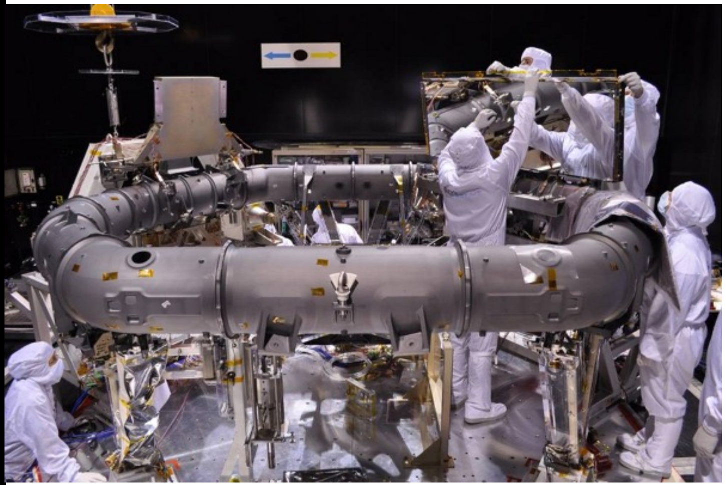

Precision: 50pico-rad, human hair at 1000km, 2cm on the moon...

SINGLE GAIA OBSERVATION = TRANSIT

Camera:

0.75 deg^2

pixel:
10x30 µm
(59x177 mas)

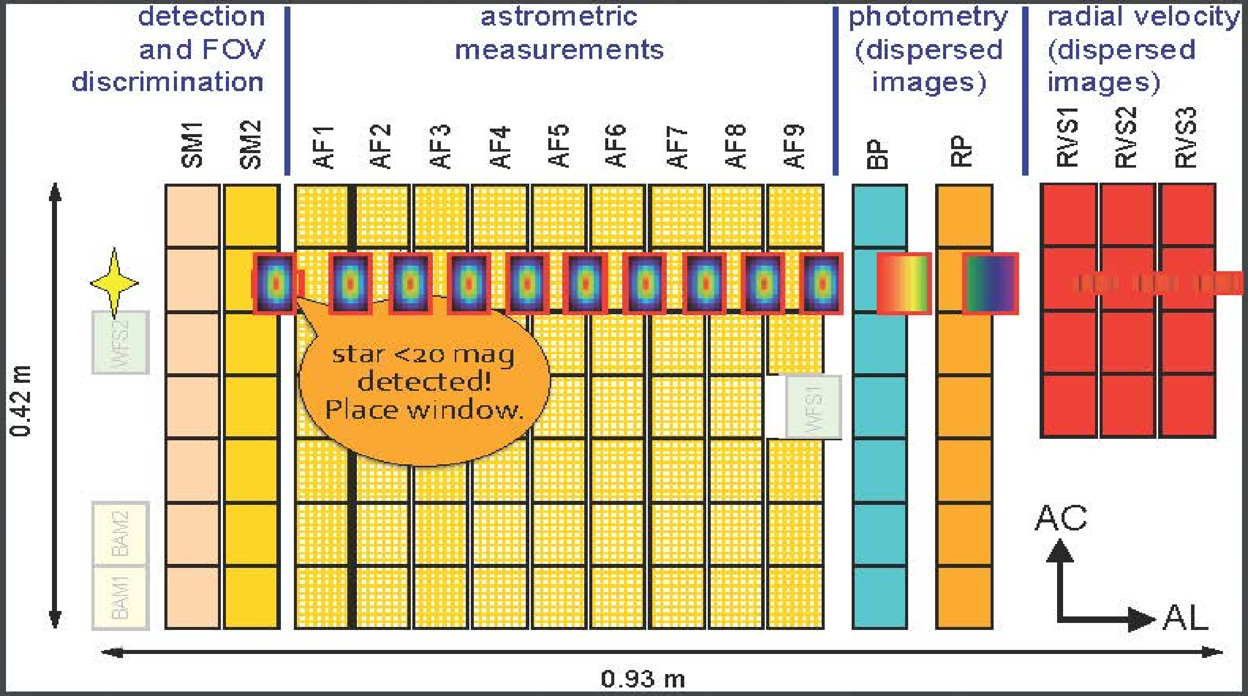

Animation by
Berry Holl,
Geneva

windows observed:

→ ~4.4 sec

→ ~45 sec

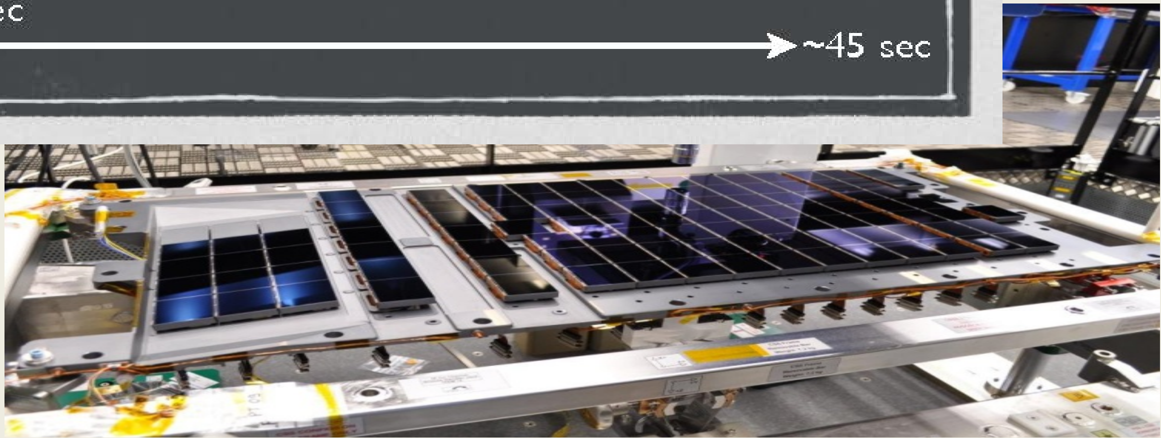

Two telescopes at a fixed large angle – from relative to absolute

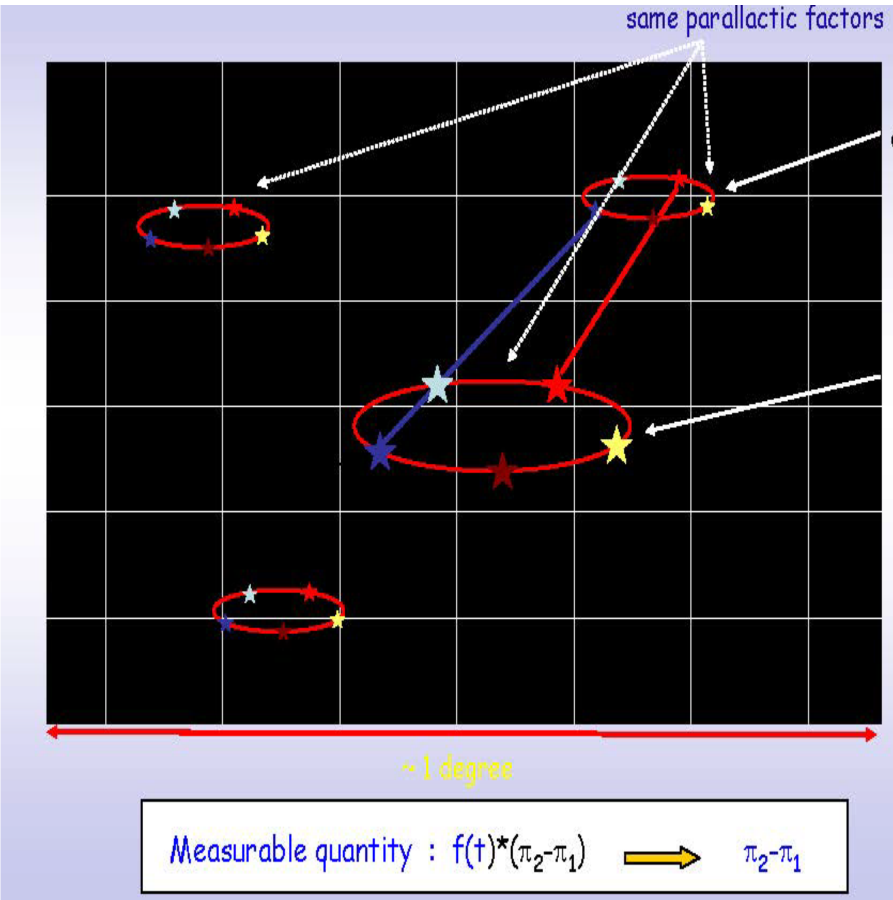

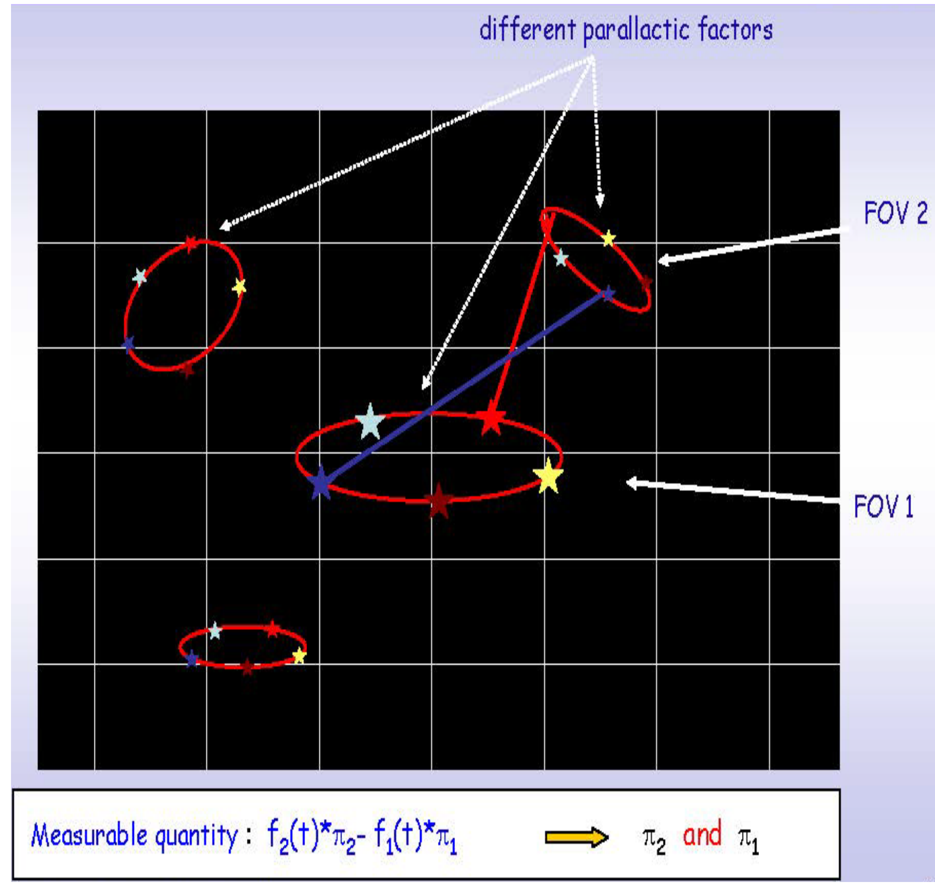

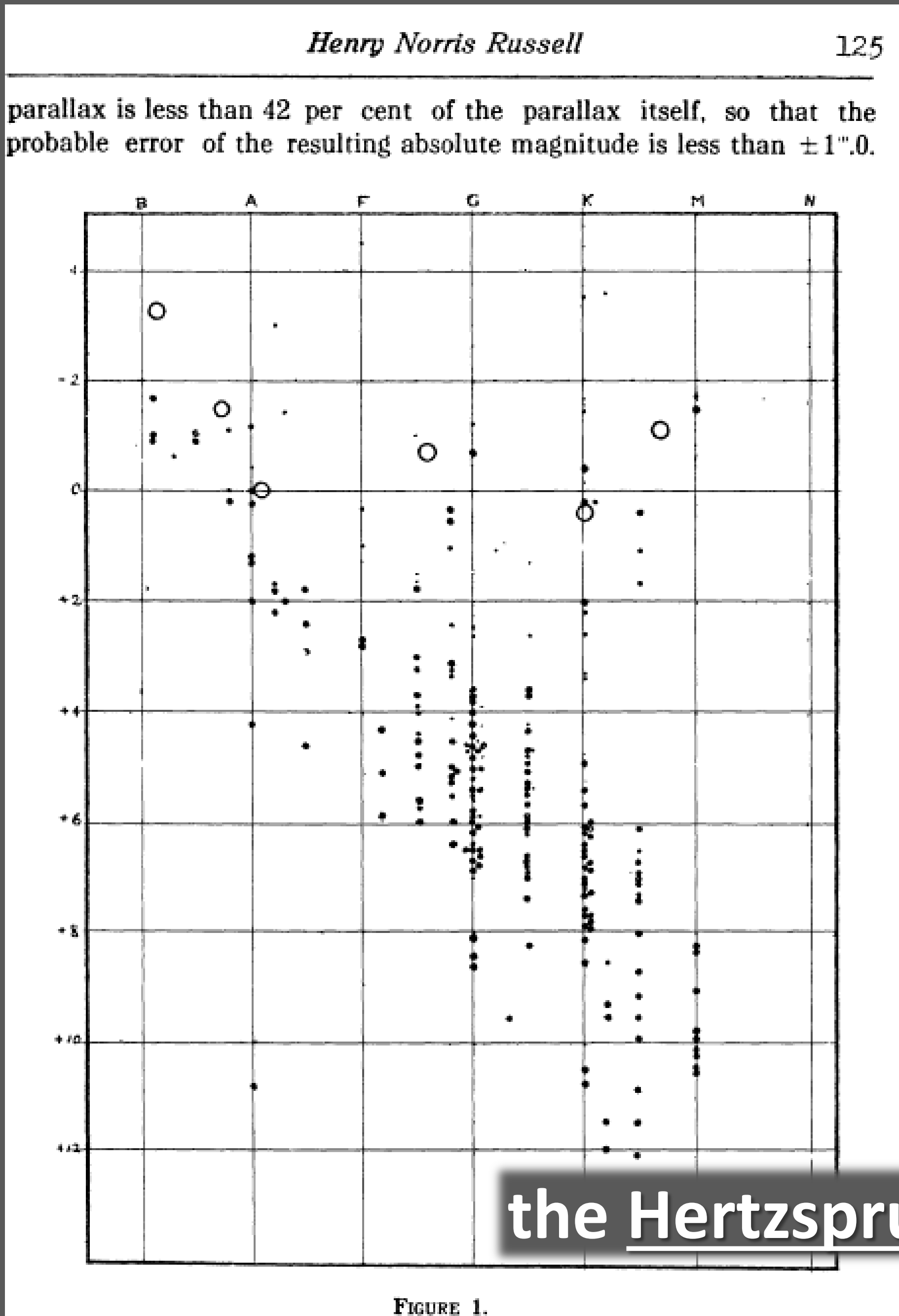

Henry Norris Russell 125

parallax is less than 42 per cent of the parallax itself, so that the probable error of the resulting absolute magnitude is less than ±1".0.

FIGURE 1.

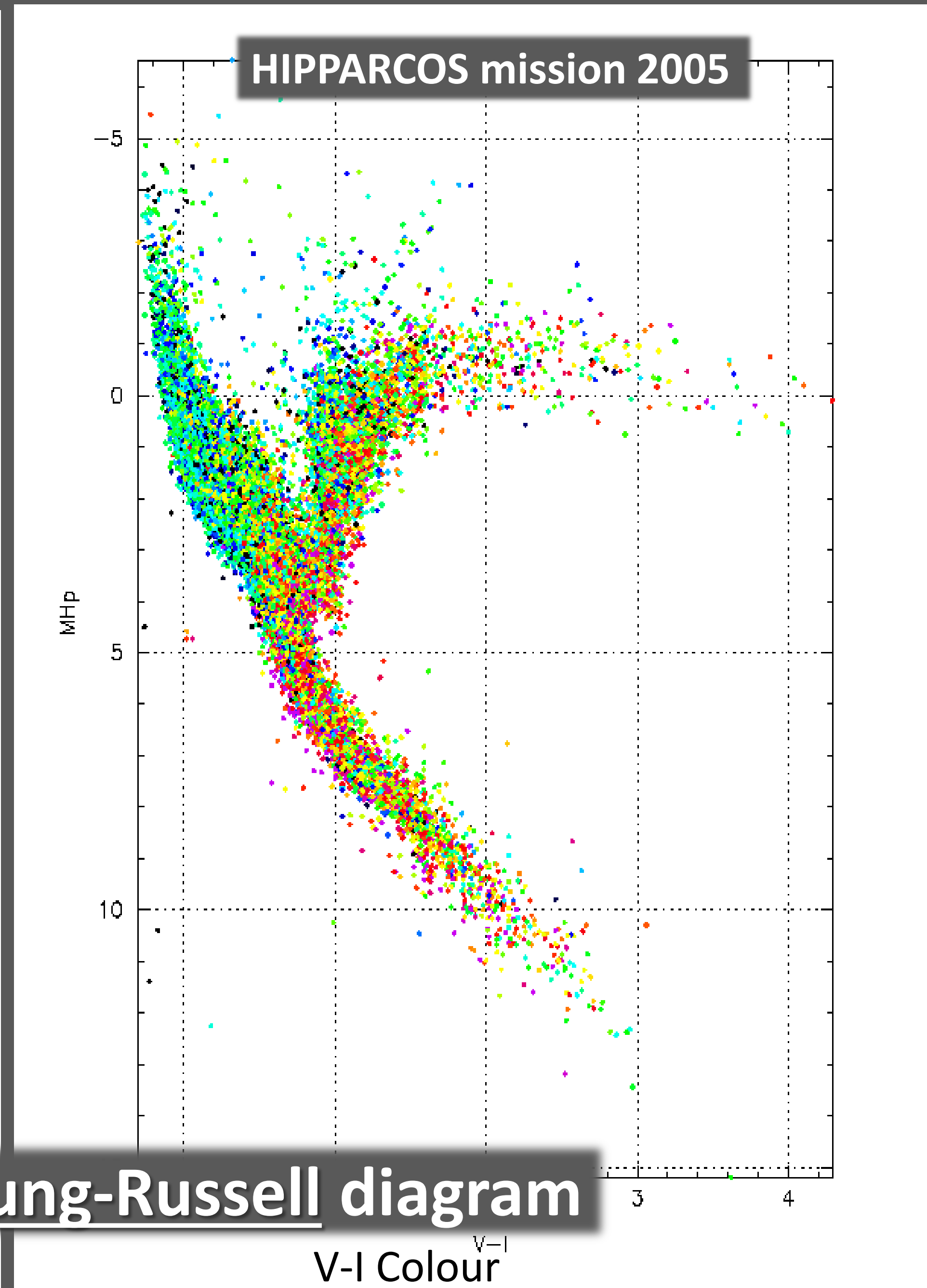

the Hertzsprung-Russell diagram

Stellar distances: Cambridge & Anne Sheepshanks

Nos. 618-619.

VOL. XXVI. ALBANY, N.Y., 1910 OCTOBER 28.

DETERMINATIONS OF STELLAR PA…

[From Photographs Taken at the Cambridge Observatory (England) by Arth…

By HENRY NORRIS RUSSELL.

The present communication contains the final results of the first series of observations for stellar parallax made at the *Cambridge Observatory*. The plans for the work* were prepared by Mr. A. R. Hinks, Chief Assistant at the Observatory, and the writer — who had been appointed a Research Assistant of the *Carnegie Institution* for the purpose of this investigation. Mr. Hinks and the writer are also jointly responsible for the photographic observations in nearly equal shares. The former contributes 43%. For the measurement and reduction of the plates, which was begun at Cambridge and completed at Princeton, and for the results and conclusions here detailed, the writer is alone responsible.

The determinations of photometric magnitude and spectrum were made at the *Harvard College Observatory*, the latter by Mrs. Fleming, and the former by Prof. E. C. Pickering, to whom the writer's most hearty thanks are due for this extremely important addition to the value of the work.

I. Methods of Observation and Reduction.

A detailed account of the methods employed in the present work, with the reasons for their adoption, is given in the paper by Mr. Hinks and the writer, already referred to. It may be summarized as follows:

The photographs were taken with the Sheepshanks Equatorial of the Cambridge Observatory† — a *coudé* telescope of the polar siderostat type, of 12 inches effective aperture and 19.3 feet focal length. The stability of this instrument, and the performance of its driving clock and electric control, were so satisfactory that no attempts were made to guide by hand.

The plates, coated on plate-glass, cover a field a little less than $1\frac{1}{2}°$ square. Four exposures were usually made on each, separated by $\frac{1}{2}$ mm. in declination. With the standard exposure of five minutes, stars are shown to the eleventh (photographic) magnitude.

separate plates we… at once — because, i… whose success depen… the same plate at th… be spoiled by the fai… conditions of the wo… ment should be begu…

All plates were t… meridian, to avoi… systematic errors,† d… tude, which may a… from instrumental c…

In order to obtain… along with the much f… were photographed t… a small patch of gelat… diminished the photographic bright… ing through it by about $5\frac{1}{2}$ magnitu… glass plate, placed just in front o… This worked very satisfactorily f… until the gelatine patch, contracting… of the glass. The observations of s… fourth magnitude were thus interrup… of a number of them had to be dete… tions at two epochs, with the aid … motions. Data concerning the ac… will be given later.

It should be an easy matter to c… free from this danger, *e.g.* one seale… plates.

* Hinks and Russell, *M.N.*, LXV., pp. 775–787.

† Described by Sir Robert Ball, *M N.*, LIX., pp. 152–155.

* The alternative method (Kapteyn's) … circumstances to systematic errors depen… See Kostinsky. *Publ. de l'Obs. Cent. Nic…* part 2, pp. 69, 138. Tikhoff. *Poulko…* p. 101.

† Called hour-angle error by Kapteyn. … No. 1, p. 68.

‡ This device is due to the writer.

§8. *The Sheepshanks Telescope.* Professor Adams died in January 1892, leaving to the Observatory a portable equatoreal by Cooke and a valuable collection of books. He was succeeded as Lowndean Professor and Director of the Observatory by Sir Robert Ball. In a memorandum to the Syndicate in March 1893, the new Director pressed for the erection of a refracting telescope suitable for stellar photography, with a view to work on stellar parallax.

The first suggestion was that it should be of 12 in. aperture and 19 ft. 7 in. focal length and that it should be carried on the same mounting as the Northumberland Telescope which could be used as a guiding telescope. It was hoped to provide the greater part of the cost from the special Sheepshanks Fund and to appeal to the public for subscriptions to meet the balance. The appeal was not successful and it was decided to look to the Sheepshanks Fund for the whole sum. Professor Stokes, Mr Newall and the Director were appointed a committee to prepare plans and on their recommendation a 12 in. triple apochromatic by Cooke was ordered in 1895. On the suggestion of Dr Common and Professor Turner, it was agreed in March 1896 to adopt a modified form of equatoreal *coudé* mounting designed by Sir Howard Grubb of Dublin.

(a) SHEEPSHANKS TELESCOPE

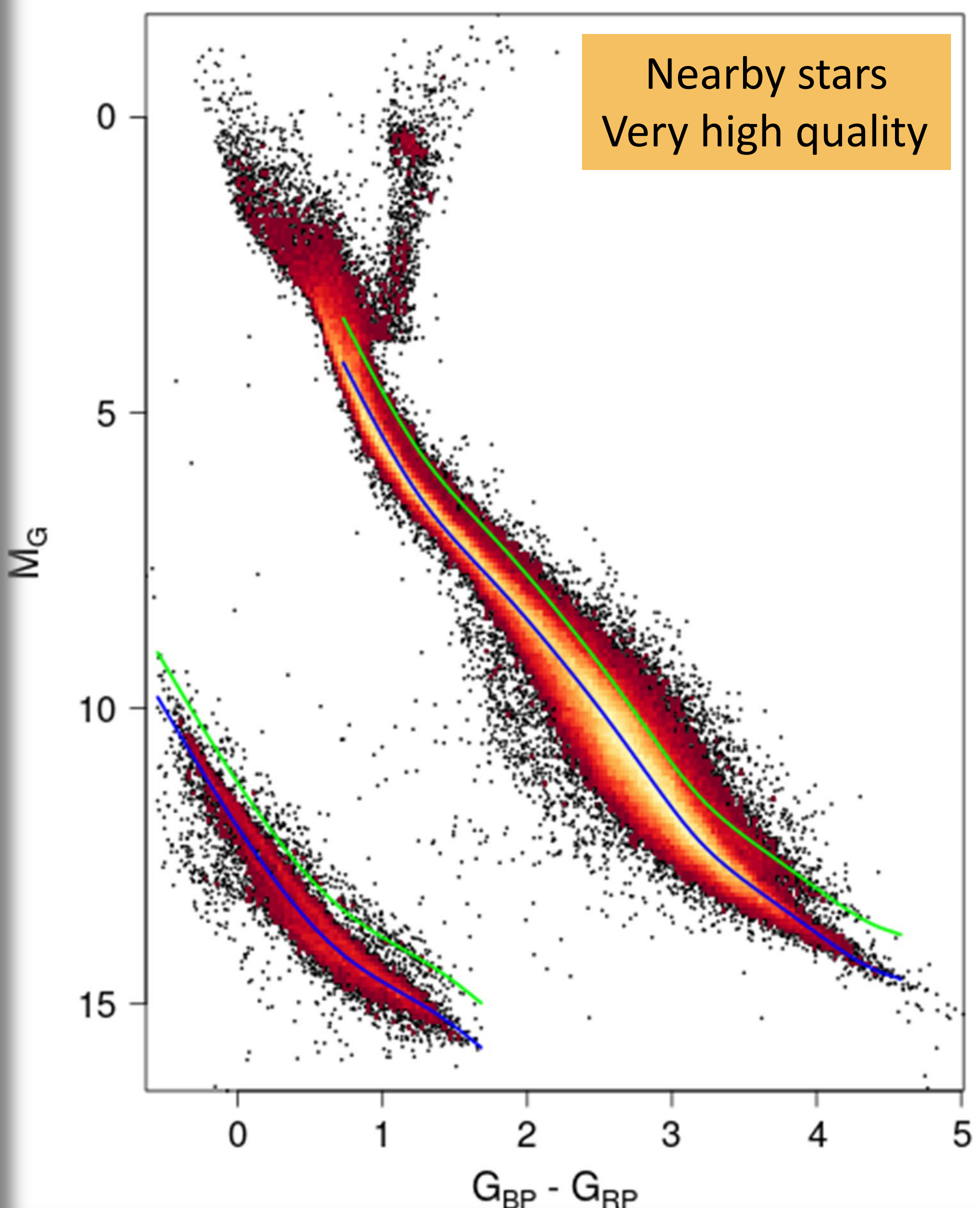

Nearby stars
Very high quality
M_G
0
5
10
15
0
1
2
3
4
5
$G_{BP} - G_{RP}$

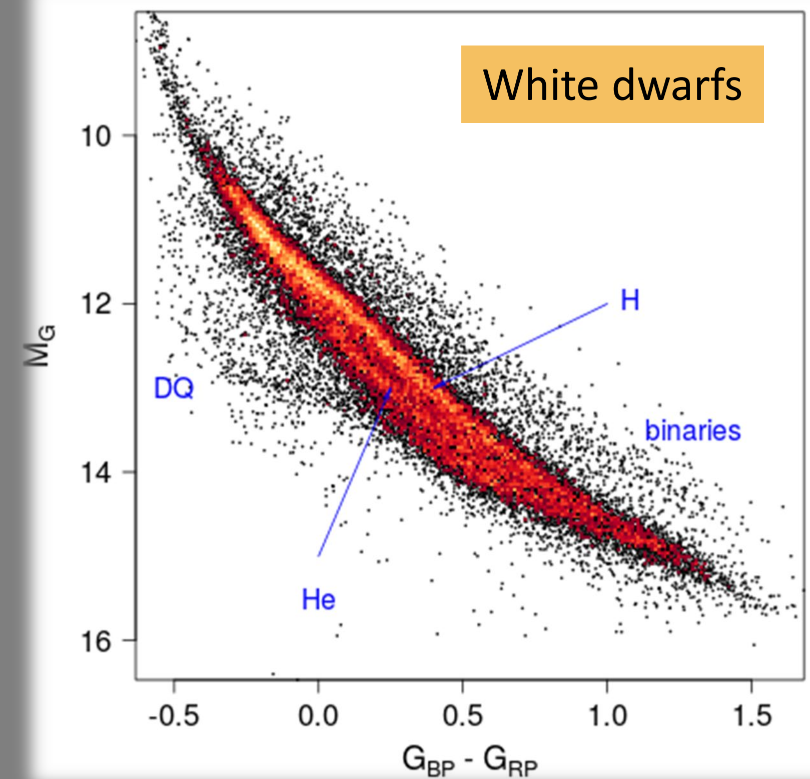

White dwarfs
M_G
10
12
14
16
DQ
H
He
binaries
-0.5
0.0
0.5
1.0
1.5
$G_{BP} - G_{RP}$

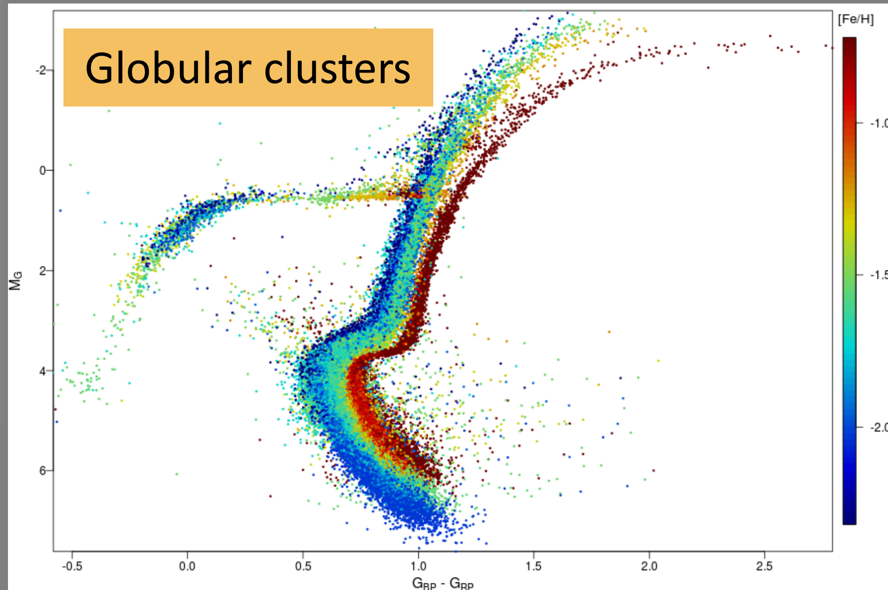

Globular clusters
[Fe/H]
-1.0
-1.5
-2.0
M_G
-2
0
2
4
6
-0.5
0.0
0.5
1.0
1.5
2.0
2.5
$G_{BP} - G_{RP}$

Gaia DR2

Gaia data are not simple to use but are worth the effort

- Random errors
- Systematic errors
- Spatially-correlated errors
- Read the data papers!

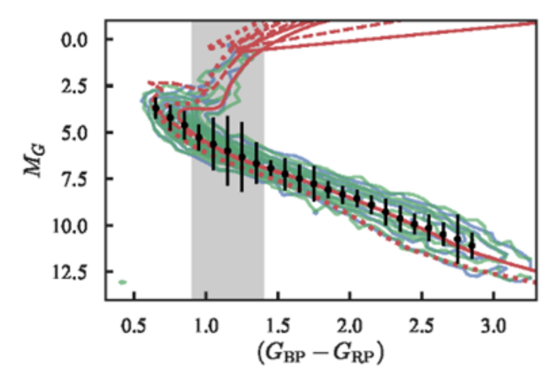

Figure 2. Colour-magnitude diagram. Contours show stars with 10 per cent parallax uncertainties (blue North, green South). Red shows three isochrones (solid: solar metallicity and 10 Gyr, dashed: −0.5 dex and 10 Gyr, dotted: solar metallicity and 3 Gyr. Black shows the median absolute magnitude and standard deviation in each considered bin. The grey region is where giant contamination could be significant.

Even with Gaia dwarf-giant
- classification is challenging

- Distance is not simply related to parallax
  - Usually one needs a model of what you are observing, and a Bayesian prior in the probability analysis.
  - Most tools are on-line in Python via Github

Real-world challenges

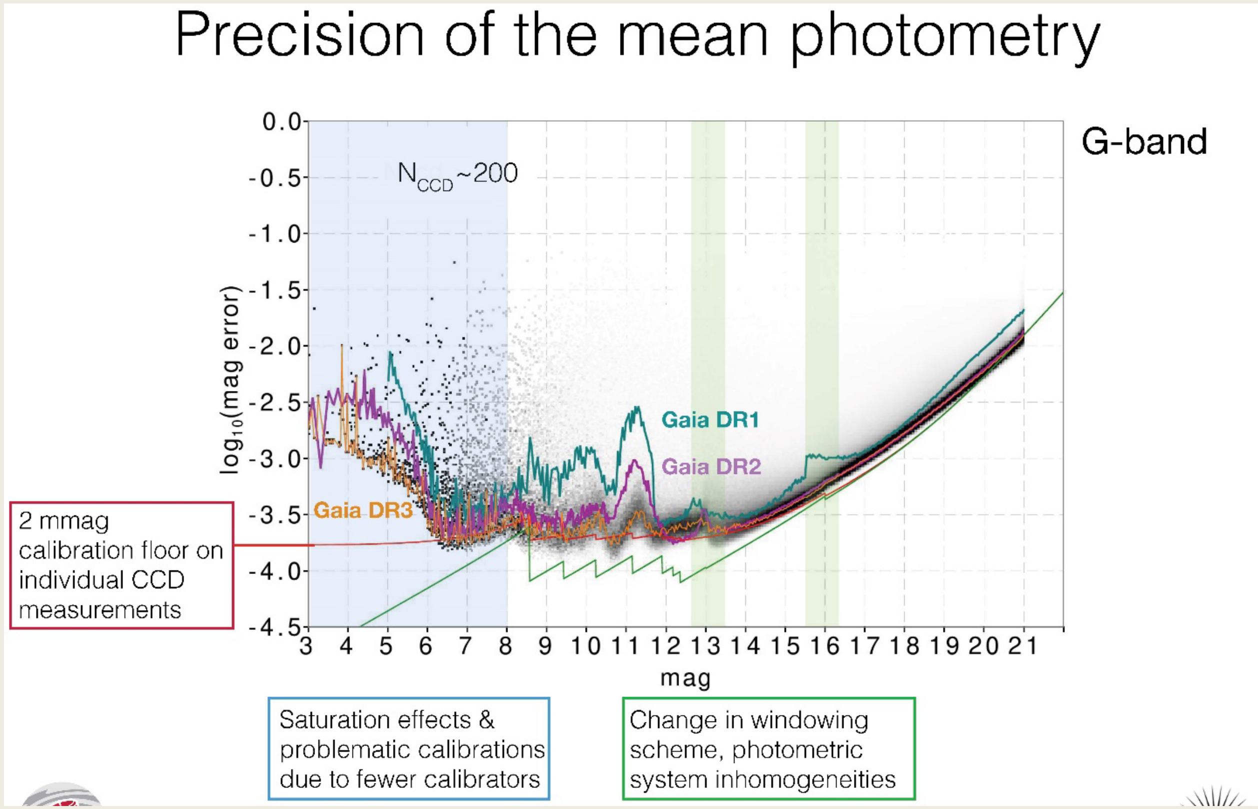

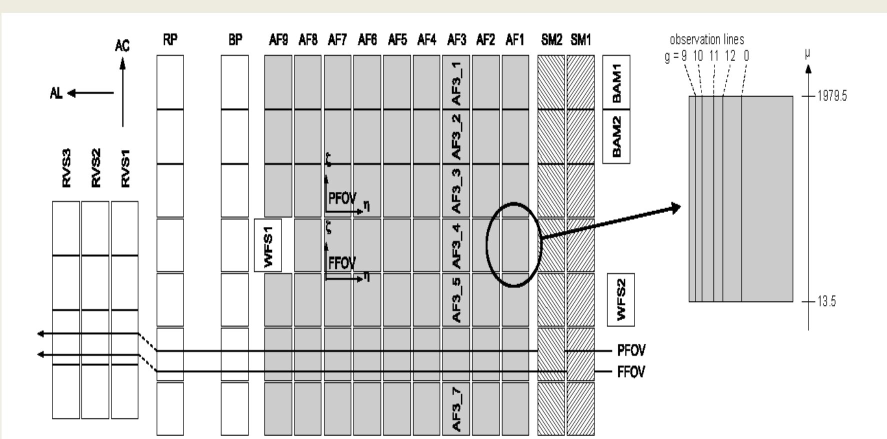

Each CCD allows several exposure times to extend dynamic range. To reduce data transmission star images are cutouts with 4 different bins. Gaia is really many different instruments, each of which must be self-calibrated.

Calibration improvement DR2 to DR3
EDR3 photometry & astrometry:3-Dec-2020

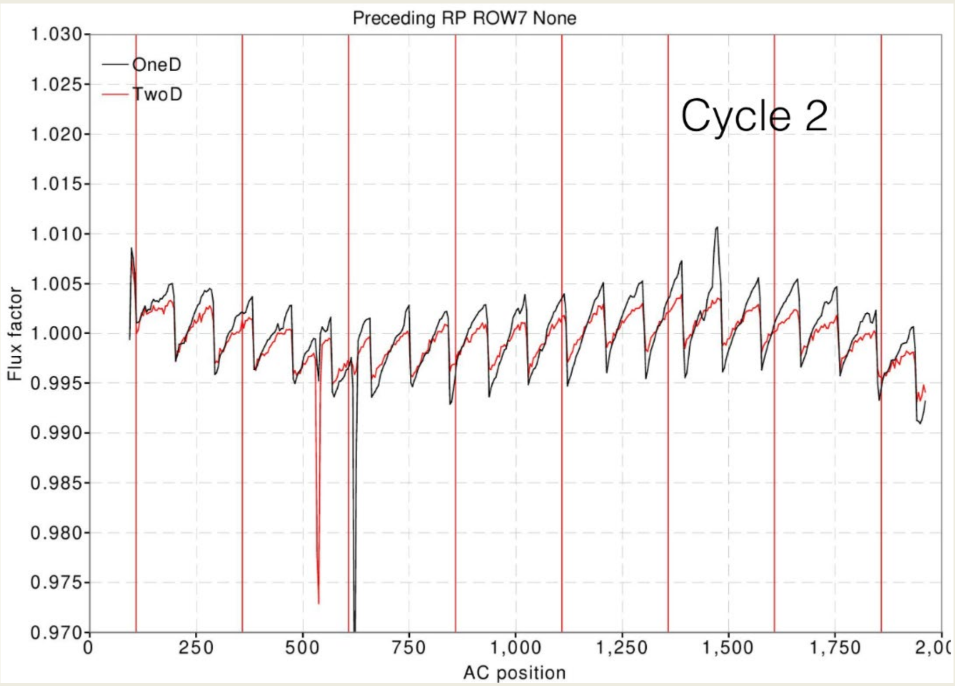

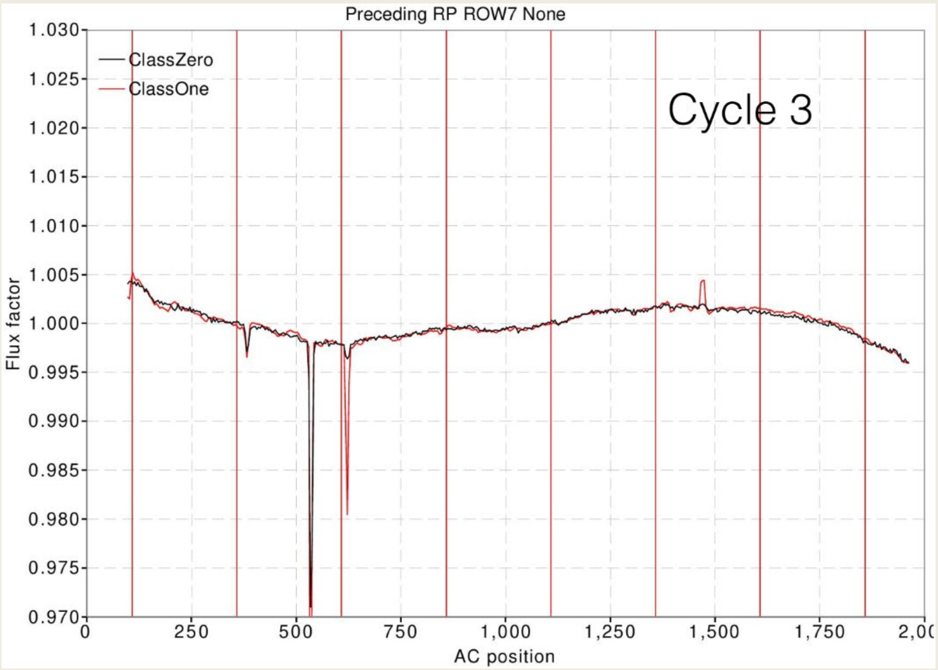

Much hard work still underway to deconvolve overlapping low-res spectra, and to deconvolve multiple marginally-resolved sources. Eventually, Gaia will have an all-sky HST-like resolution.

What is coming later: DR3 mid-2022

DR3: New products

Epoch photometry

- Variable light-curves (more variability types, up to ~7 million photometric light-curves and classifications)
- Gaia Andromeda Photometric Survey (GAPS) (G, G_{BP}, G_{RP} light-curves for ~1M sources)

BP/RP low-resolution spectroscopy and related products

- Internally calibrated mean BP and RP spectra for at least 100M sources
- External calibration of the BP and RP mean instrument
- Astrophysical parameters
- Reflectances from BP/RP spectra of asteroids

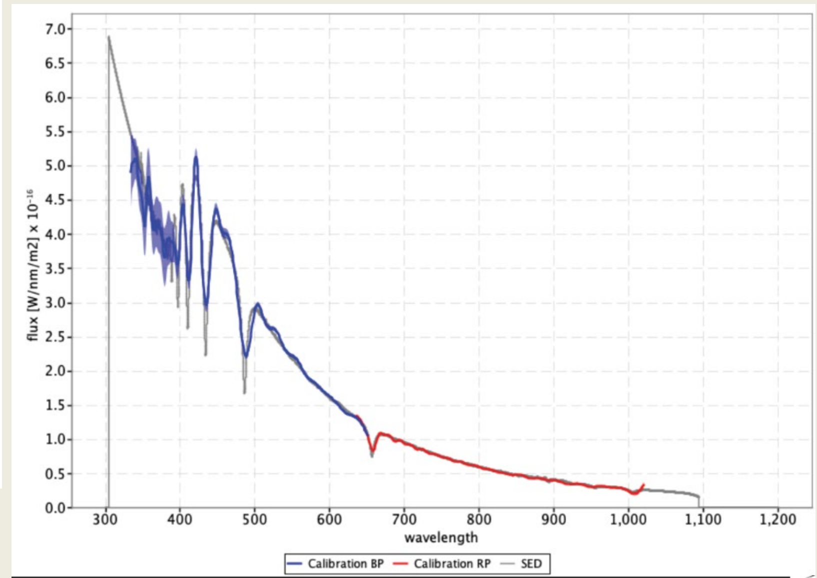

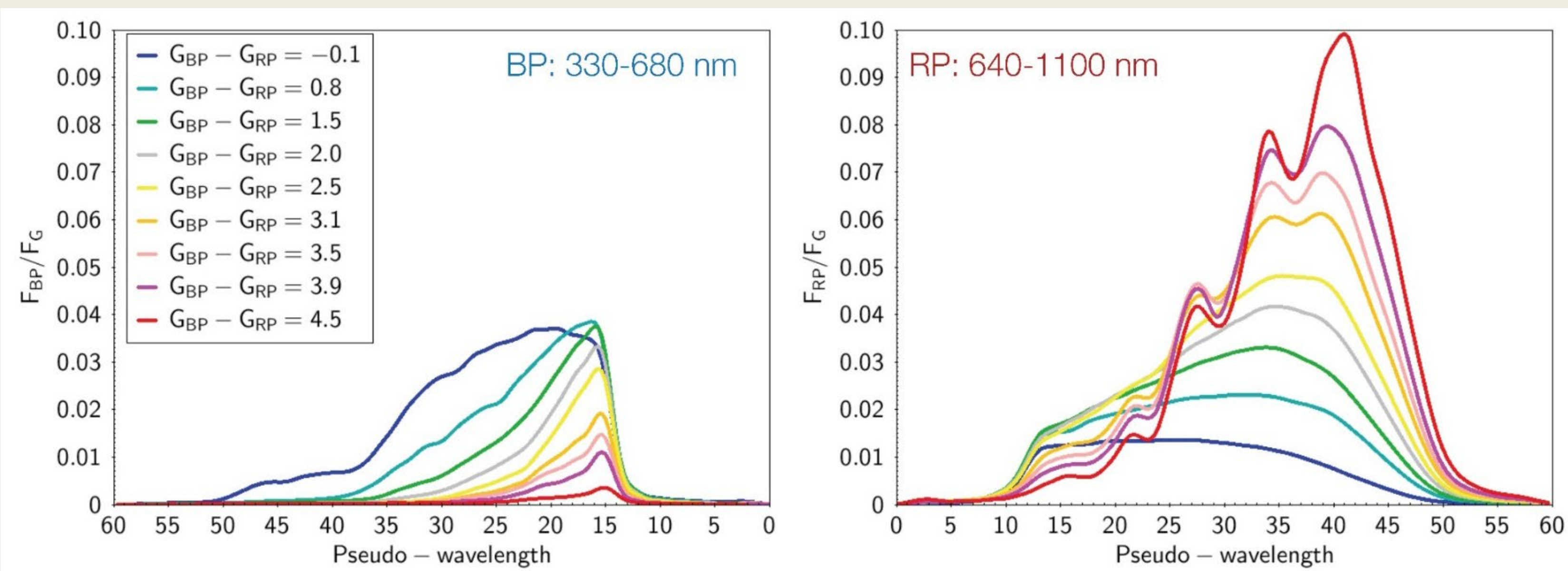

DR3: Asteroid reflectances

M. Delbo, L. Galluccio, F. De Angeli, T. Pauwels, F. Mignard, A. Cellino, P. Tanga

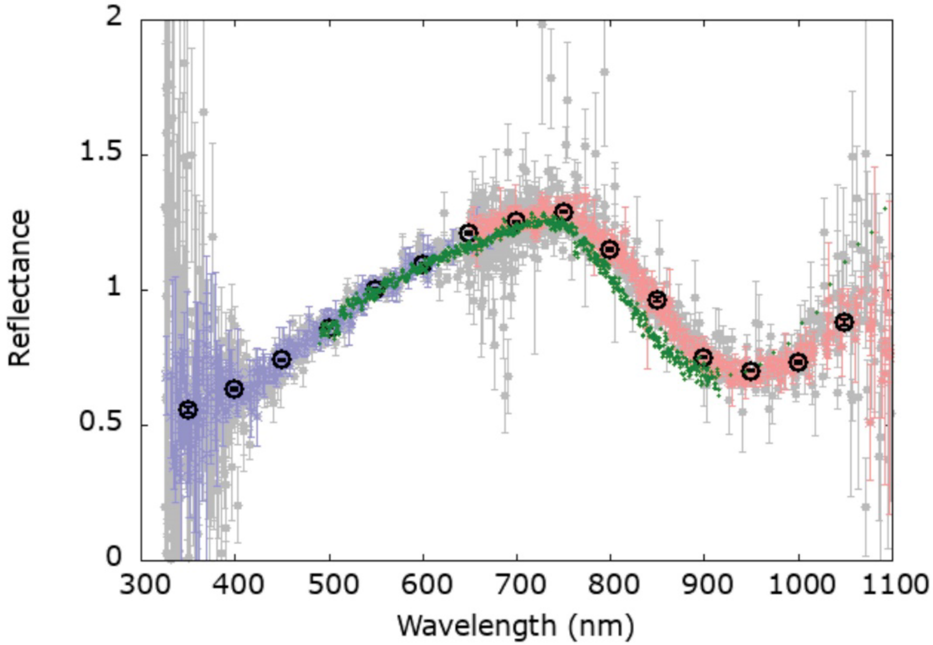

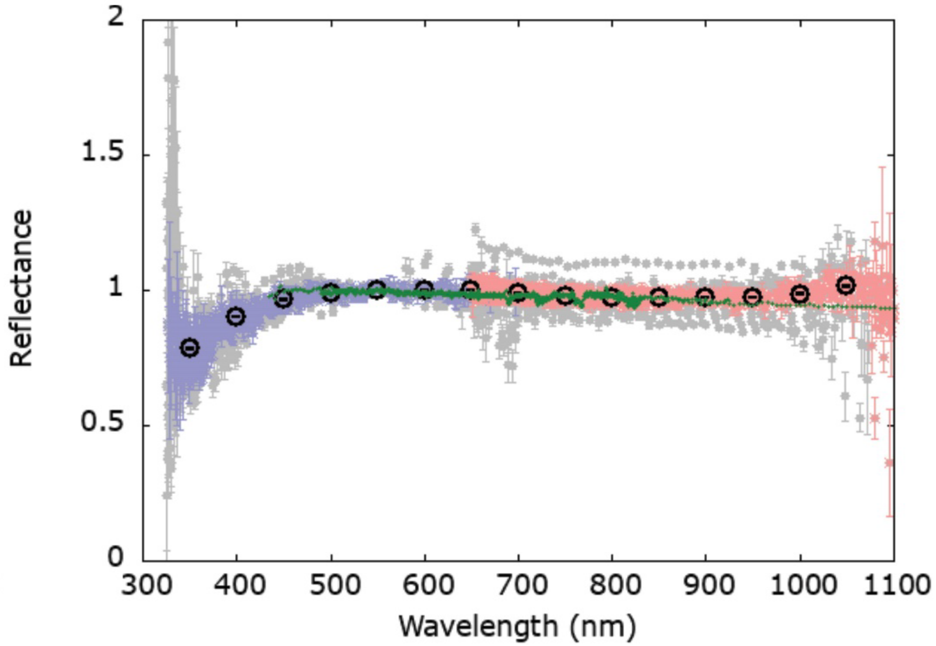

Gaia DR3 will include **reflectances** for several thousand asteroids computed from BP/RP epoch spectra. This will be a unique catalogue for its homogeneity and size.

The Gaia reflectances will extend the wavelength coverage in the range 350-500nm which is important to understand the chemical composition of these objects and is not covered by ground-based data.

All the data: TIME DOMAIN

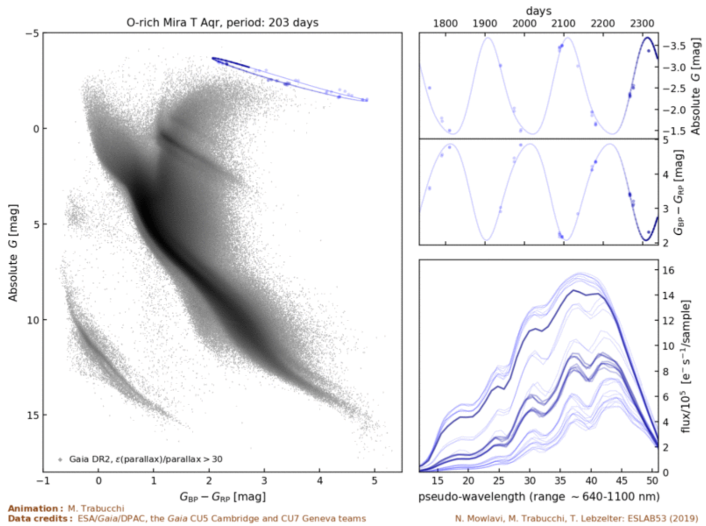

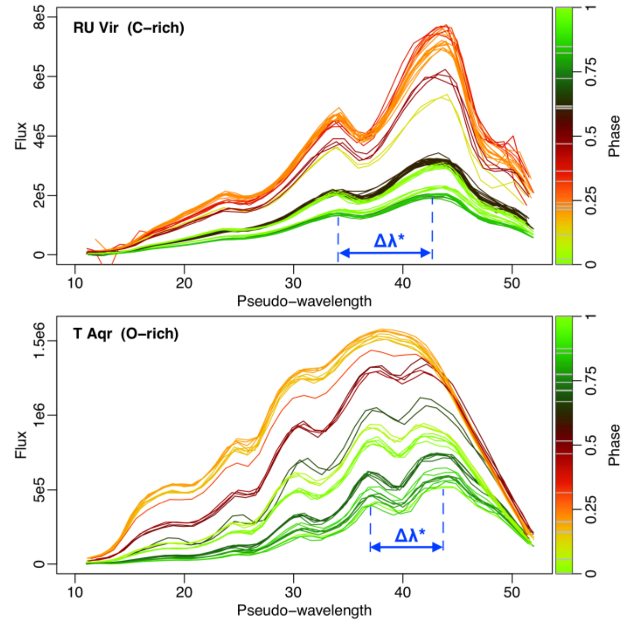

Image credits: ESA/Gaia/DPAC, Mowlavi et al.

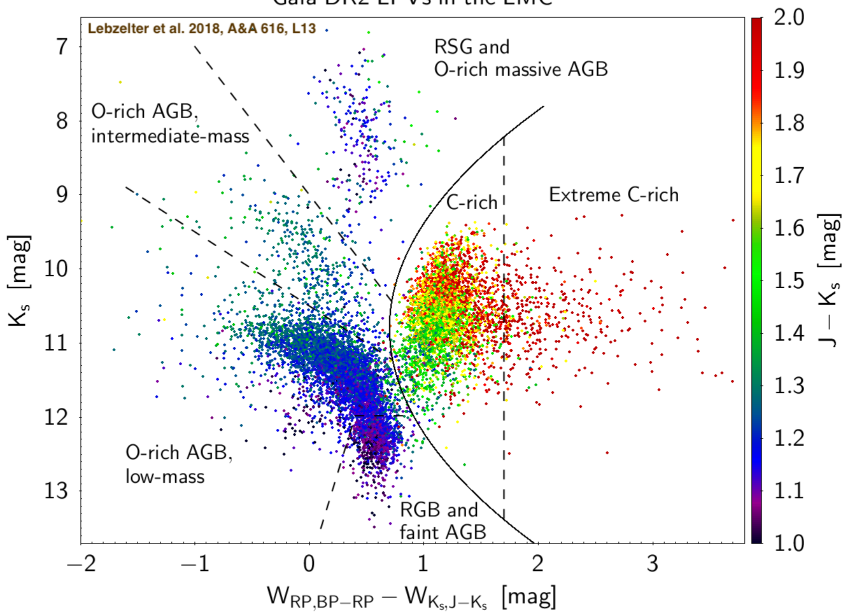

Gaia16aeg

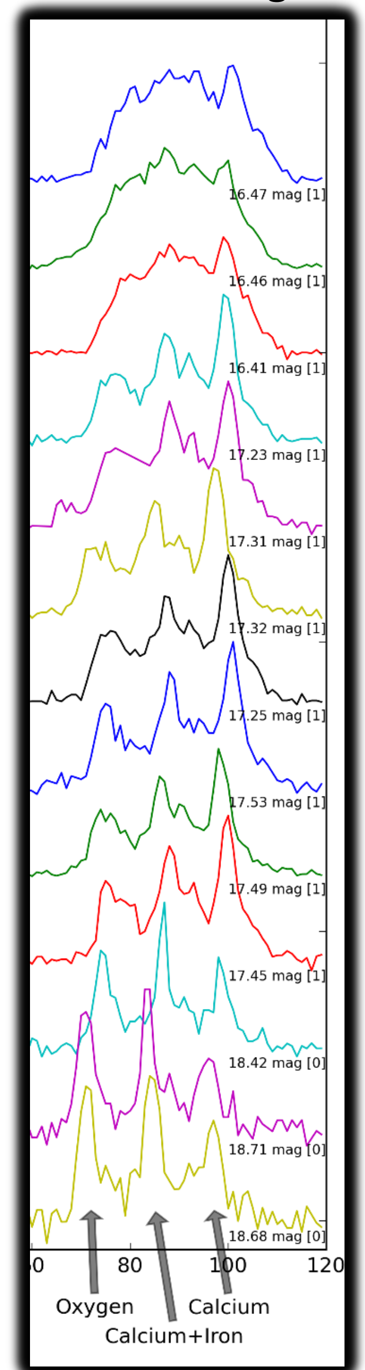

Time Domain: Be stars with Gaia

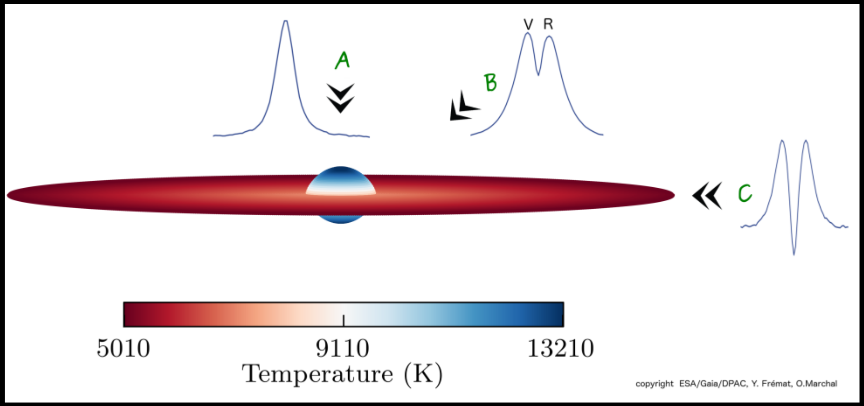

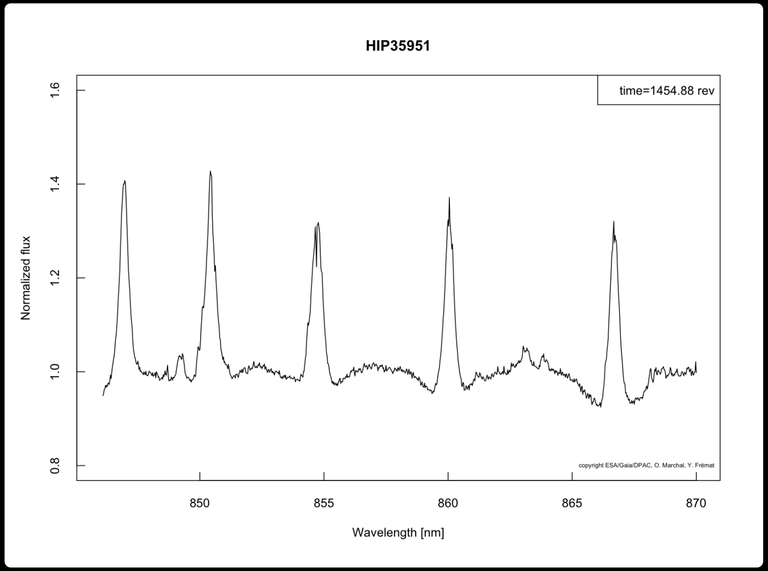

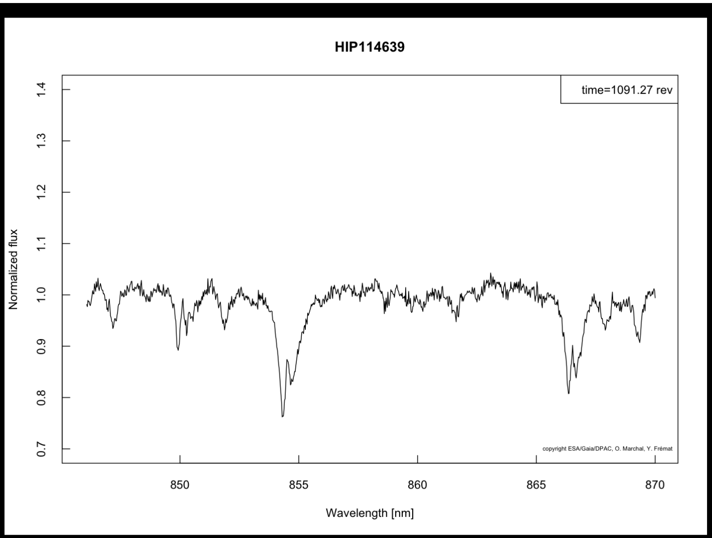

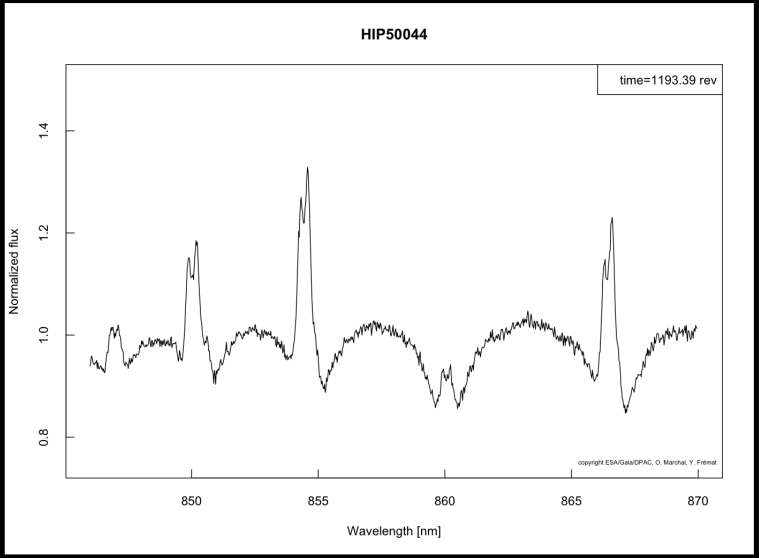

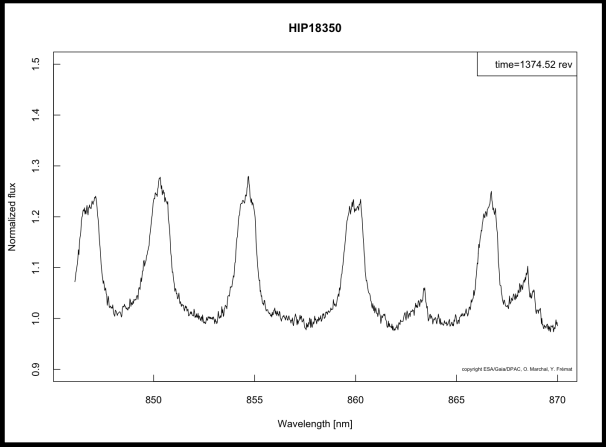

Gaia16aye - a background star whose light is lensed by the space-time distortion of a binary – two stars exactly lined up between us and the star.

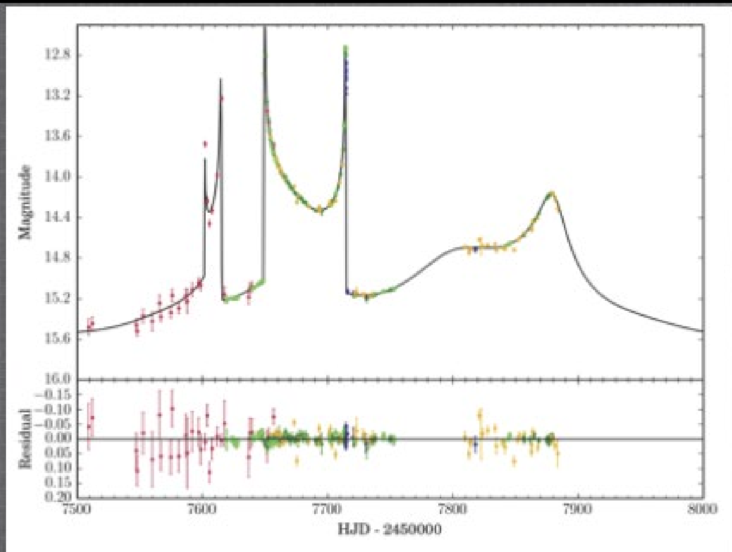

25000 observations from >60 telescopes

GaiaAlerts network

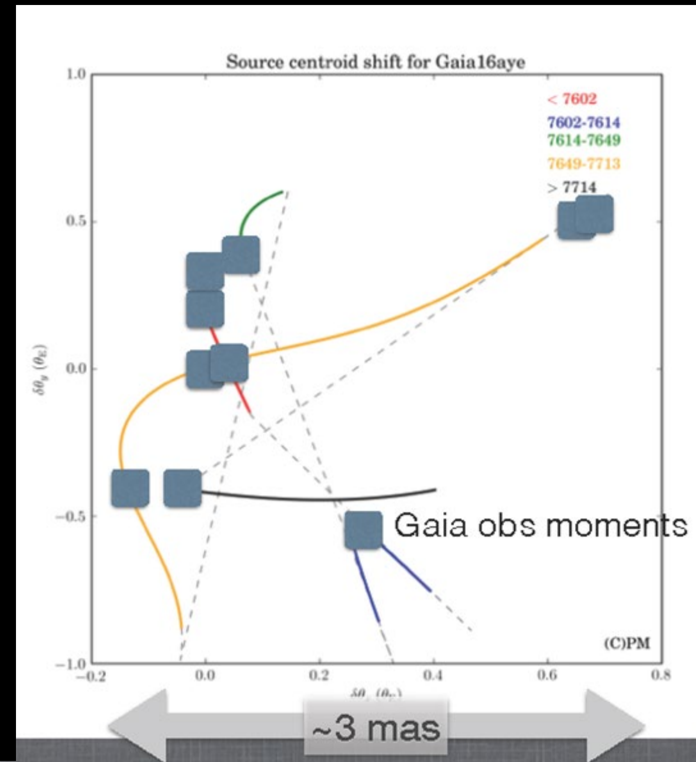

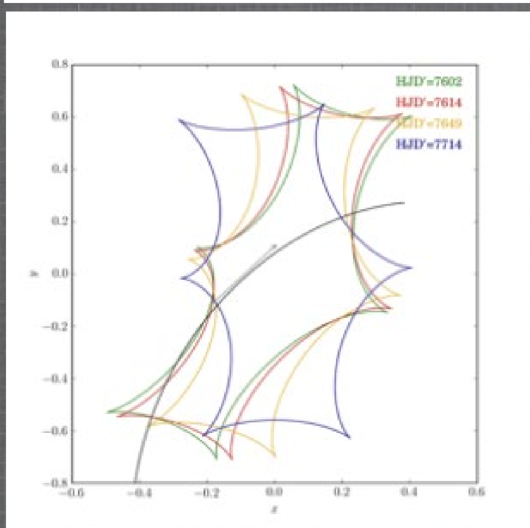

A&A 693 A98 2020

Local dark matter density

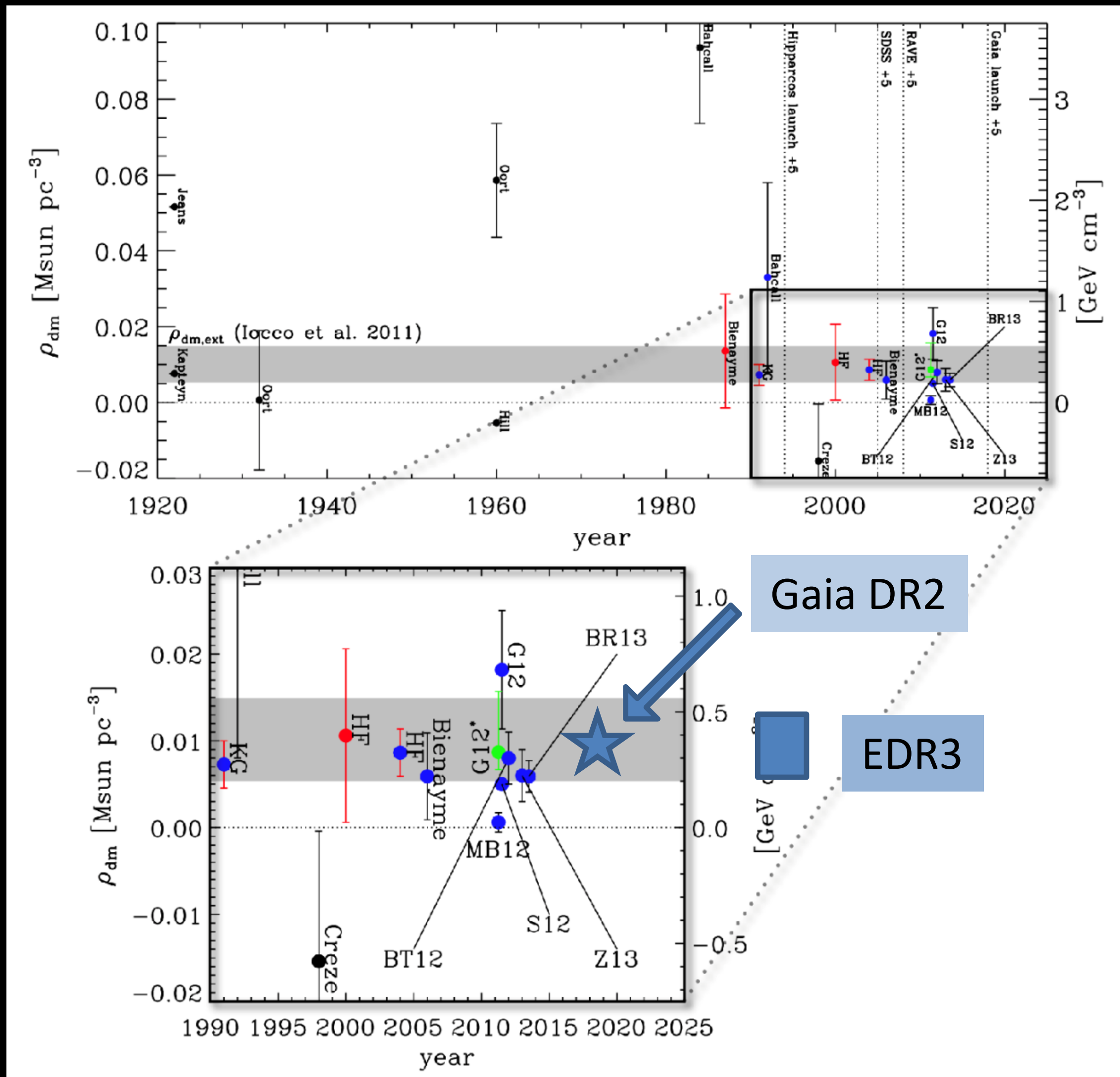

arXiv: 1404.1938
arXiv: 1605.04909

Local dark matter density measures have been consistent since Kuijken & Gilmore 1989.
Did Gaia change all that?

Local dark matter density: will Gaia make a difference?

Consider “halo” DM and a possible dissipative thin disk of DM

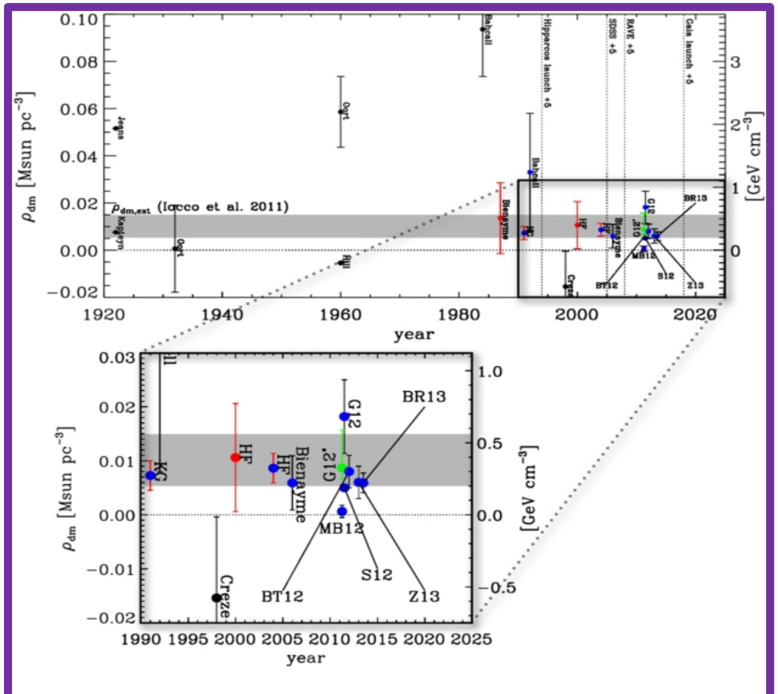

0.01 Ms/pc3 = 0.38GeV/cc

McKee etal 2015

Table 4. Local Density of Dark Matter

Reference	Σ_z ($M_\odot$ pc^{-2})	$\Sigma_{b,z}$ ($M_\odot$ pc^{-2})	ρ_{DM} ($M_\odot$ pc^{-3})	ρ_{DM} (This work)[a] ($M_\odot$ pc^{-3})
Kuijken & Gilmore (1991)	$\Sigma_{1.1} = 73.5 \pm 6$[b]	$\Sigma_{b1.1} = 48 \pm 8$	0.010[c]	0.0135 ± 0.0031
Bovy & Rix (2013)	$\Sigma_{1.1} = 68 \pm 4$	$\Sigma_b = 51 \pm 4$[d]	0.008	0.0110 ± 0.0024
Zhang et al. (2013)	$\Sigma_{1.0} = 69 \pm 6$[b]	$\Sigma_{b1.0} = 55 \pm 5$	0.0065	0.0130 ± 0.0034
Bienaymé et al. (2014)[e]	$\Sigma_{1.0} = 70.5 \pm 1$[b]	$\Sigma_{b1.0} = 43 \pm 4$	0.0143	0.0137 ± 0.0017

[a]From Equation (47) using the total surface density from the reference and the baryonic surface densities found here, $\Sigma_{b1.1} = 43.8 \pm 3.4\, M_\odot$ pc^{-2} and $\Sigma_{b1.0} = 43.1 \pm 3.3\, M_\odot$ pc^{-2}.

[b]Inferred from value of $K_z/(2\pi G)$ given in reference using Equation (54) with $\alpha = 0$.

[c]Inferred from their values for $\Sigma_{1.1}$ and $\Sigma_{b1.1}$.

[d]The authors neglected the difference between Σ_b and $\Sigma_{b1.1}$ (Bovy, private communication).

[e]For their scale height of 300 pc, $\Sigma_{b1.0} \simeq \Sigma_{b1.1} \simeq 43\, M_\odot$ pc^{-2}.

Table 5. The Oort Limit

Reference	ρ_0 ($M_\odot$ pc^{-3})
Oort (1960)[a]	0.15 ± 10%
Kuijken & Gilmore (1989c)[a,b]	0.11 − 0.29
Holmberg & Flynn (2000)	0.102 ± 0.010
Garbari et al. (2012)	$0.120^{+0.016}_{-0.019}$
Bienaymé et al. (2014)	0.091 ± 0.006
This work	0.097 ± 0.013

[a]Pre-*Hipparcos* estimates.

[b]The intent of this work was to show that the estimation of the Oort limit depends on the star sample analyzed; the lower value corresponds to the estimate using a subsample of F8 dwarfs, whereas the upper one corresponds to a subsample of F5 dwarfs.

Figure 2 from The local dark matter density
J I Read 2014 J. Phys. G: Nucl. Part. Phys. 41 063101 doi:10.1088/0954-3899/41/6/063101

Local Dark Matter density derives from the vertical pressure gradient

$$\frac{1}{r\nu_i}\frac{\partial}{\partial r}\left(r\nu_i\sigma_{rz;i}\right)+\frac{1}{r\nu_i}\frac{\partial}{\partial\phi}\left(\nu_i\sigma_{\phi z;i}\right)+\frac{1}{\nu_i}\frac{d}{dz}\left(\nu_i\sigma^2_{z;i}\right)=-\frac{d\Phi}{dz},$$

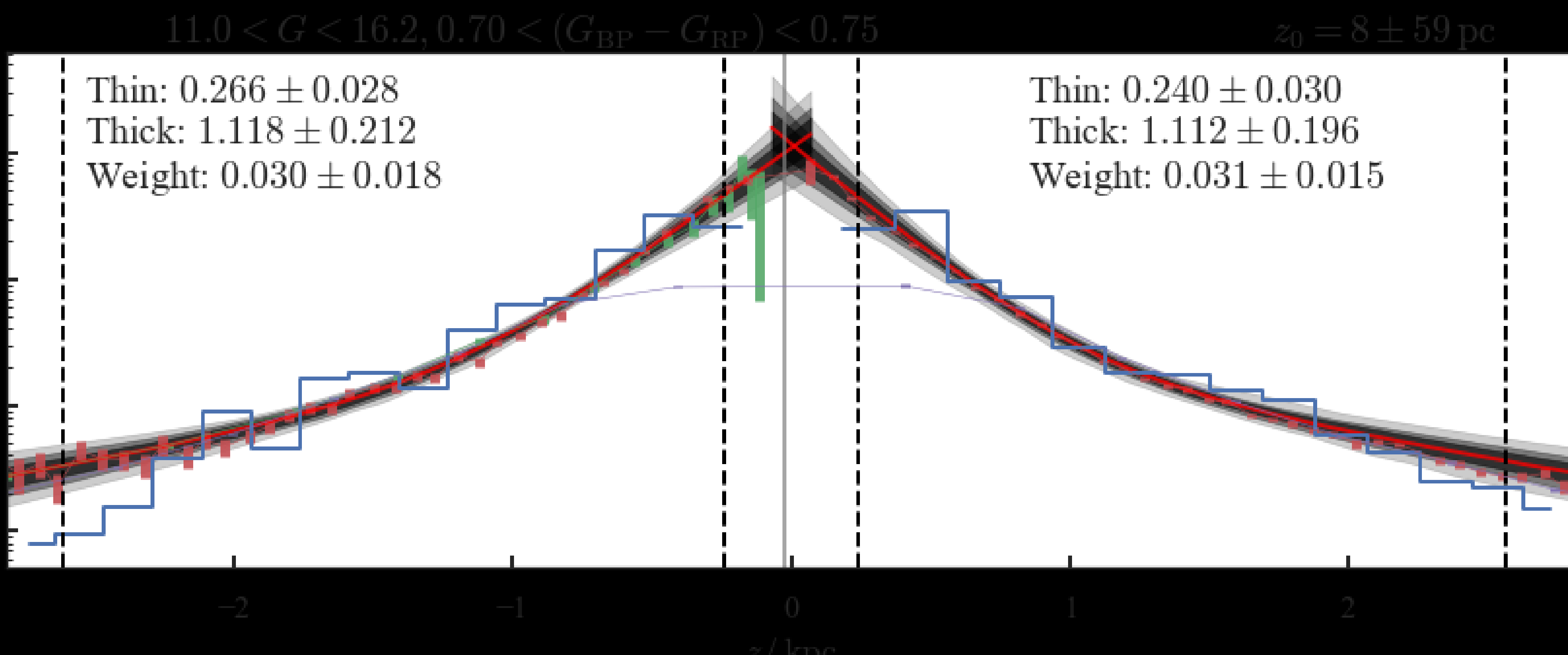

Gilmore-Reid – Green points

Juric etal - Red points

Raw counts - histogram

Black curves - bayesian reconstruction

Red curve – double exponential GR fit

A dynamically young and perturbed Milky Way disk

T. Antoja[1]*, A. Helmi[2], M. Romero-Gómez[1], D. Katz[3], C. Babusiaux[3,4], R. Drimmel[5], D. W. Evans[6], F. Figueras[1], E. Poggio[5,7], C. Reylé[8], A. C. Robin[8], G. Seabroke[9] & C. Soubiran[10]

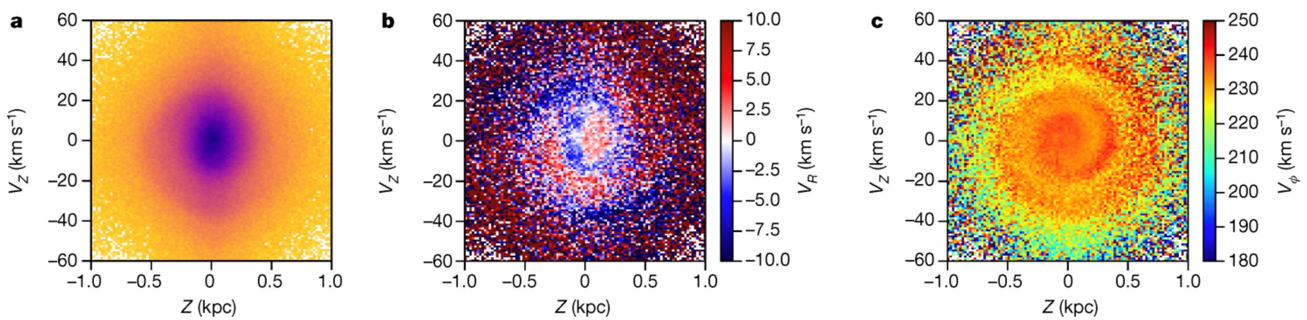

Fig. 1 | Vertical positions and velocities of the stars. The plots show the distribution of stars in the vertical position–velocity (Z–V_Z) plane from our sample of Gaia data for stars with Galactocentric radii of 8.24 kpc $< R <$ 8.44 kpc. **a**, Two-dimensional histogram in bins of $\Delta Z = 0.02$ kpc and $\Delta V_Z = 1$ km s^{-1}, with the darkness of the colour scale proportional to the number of stars. **b**, Z–V_Z plane coloured as a function of median radial velocity V_R in bins of $\Delta Z = 0.02$ kpc and $\Delta V_Z = 1$ km s^{-1}. **c**, Same as **b**, but for the azimuthal velocity V_ϕ. V_R and V_ϕ are positive towards the Galactic anticentre and the direction of Galactic rotation, respectively.

External perturbers: Sgr? Or??

The origin of the Gaia phase-plane spiral

James Binney* and Ralph Schönrich
Rudolf Peierls Centre for Theoretical Physics, Clarendon Laboratory, Oxford, OX1 3PU, UK

27 July 2018

ABSTRACT
A simple model is presented of the formation of the spiral the (z, v_z) phase plane of solar-neighbourhood stars that was recently discovered in Gaia data. The key is that the frequency Ω_z at which stars oscillate vertically depends on angular momentum about the z axis in addition to the amplitude of the star's vertical oscillations. Spirals should form in both $\langle v_\phi \rangle$ and $\langle v_R \rangle$ whenever a massive substructure, such as the Sgr dwarf galaxy, passes through the Galactic plane. The model yields similar spirals to those observed in both $\langle v_\phi \rangle$ and $\langle v_R \rangle$. The primary driver is the component of the tidal force that lies in the plane. We investigate the longevity of the spirals and the mass of the substructure, but the approximations inherent in the model make quantitative results unreliable. The work relies heavily on a self-consistent, multi-component model of our Galaxy produced by the AGAMA package for $f(\mathbf{J})$ modelling.

Widmark et all arXiv:2105:14030. Non-equilibrium dynamical modelling

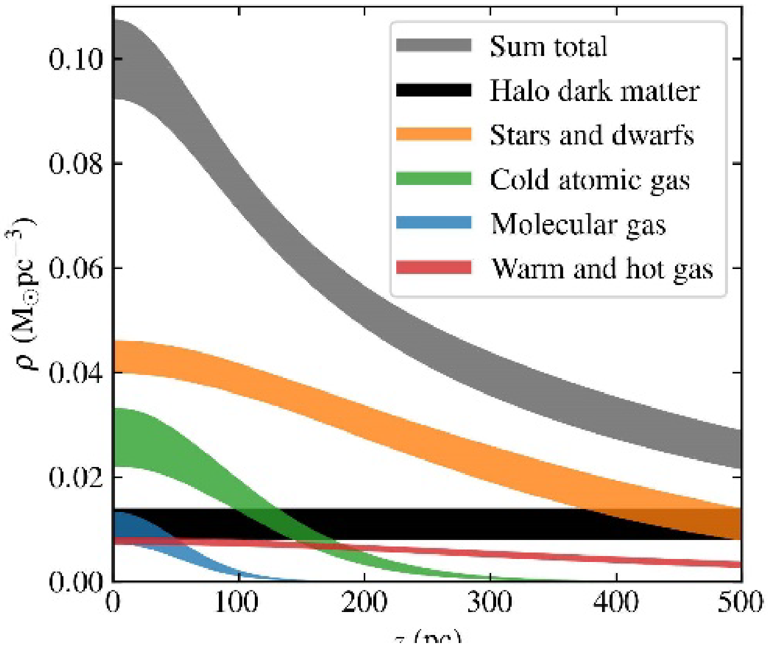

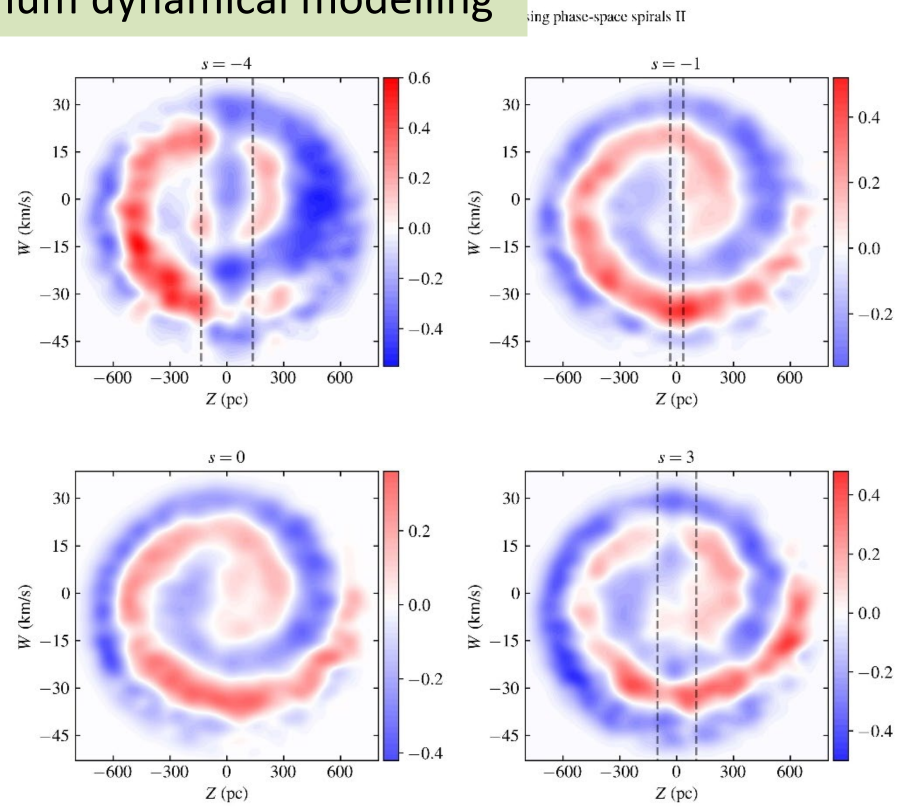

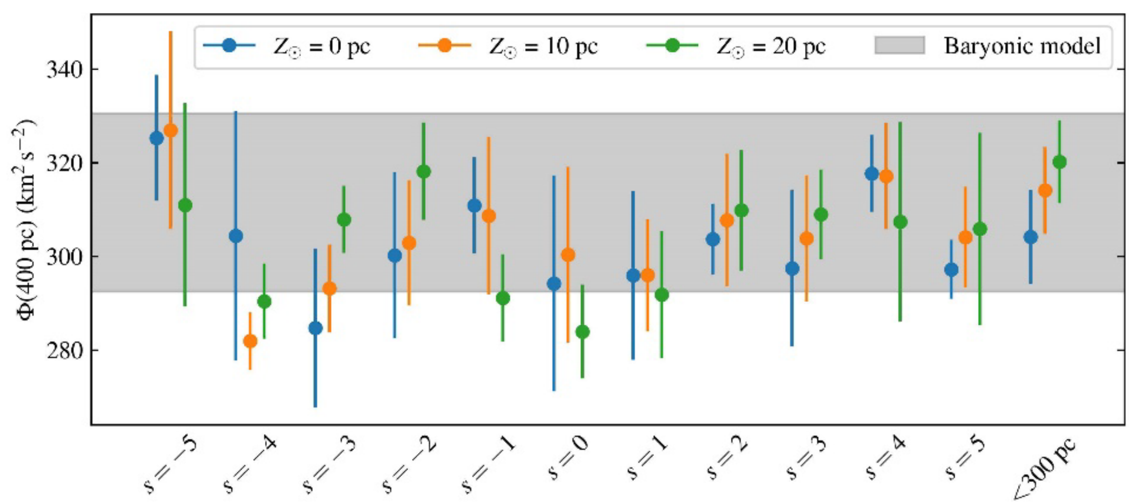

Kepler ages extend dimensionality – and the challenge

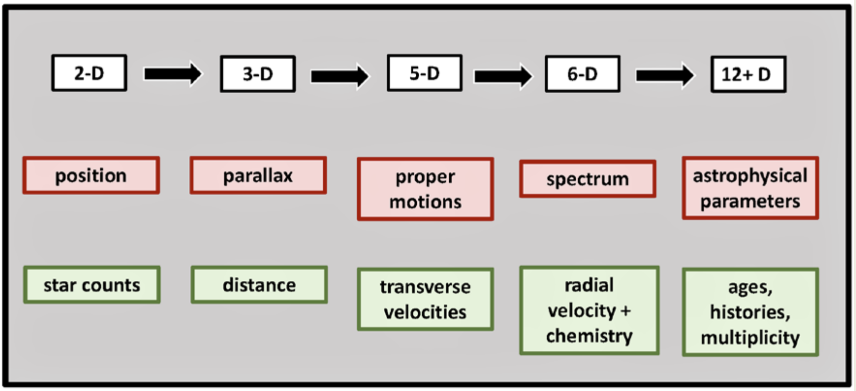

Remarkable similarity of diverse enrichments

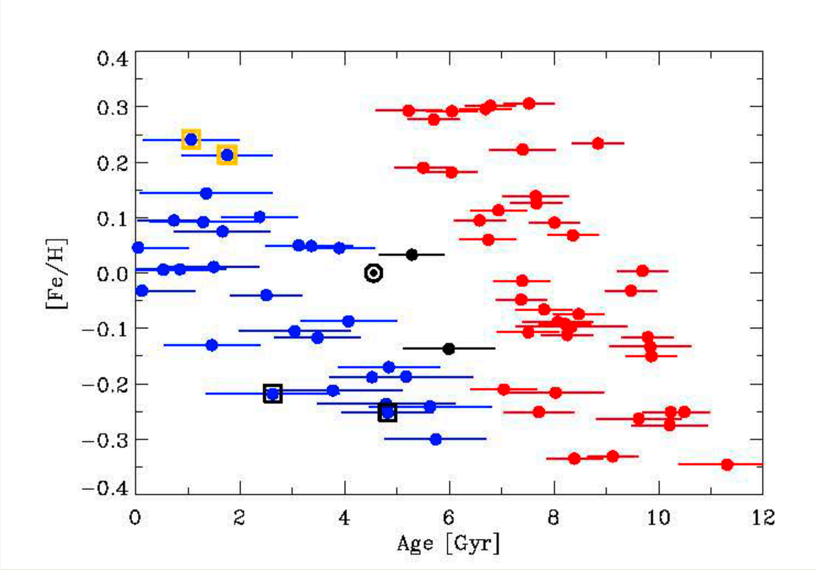

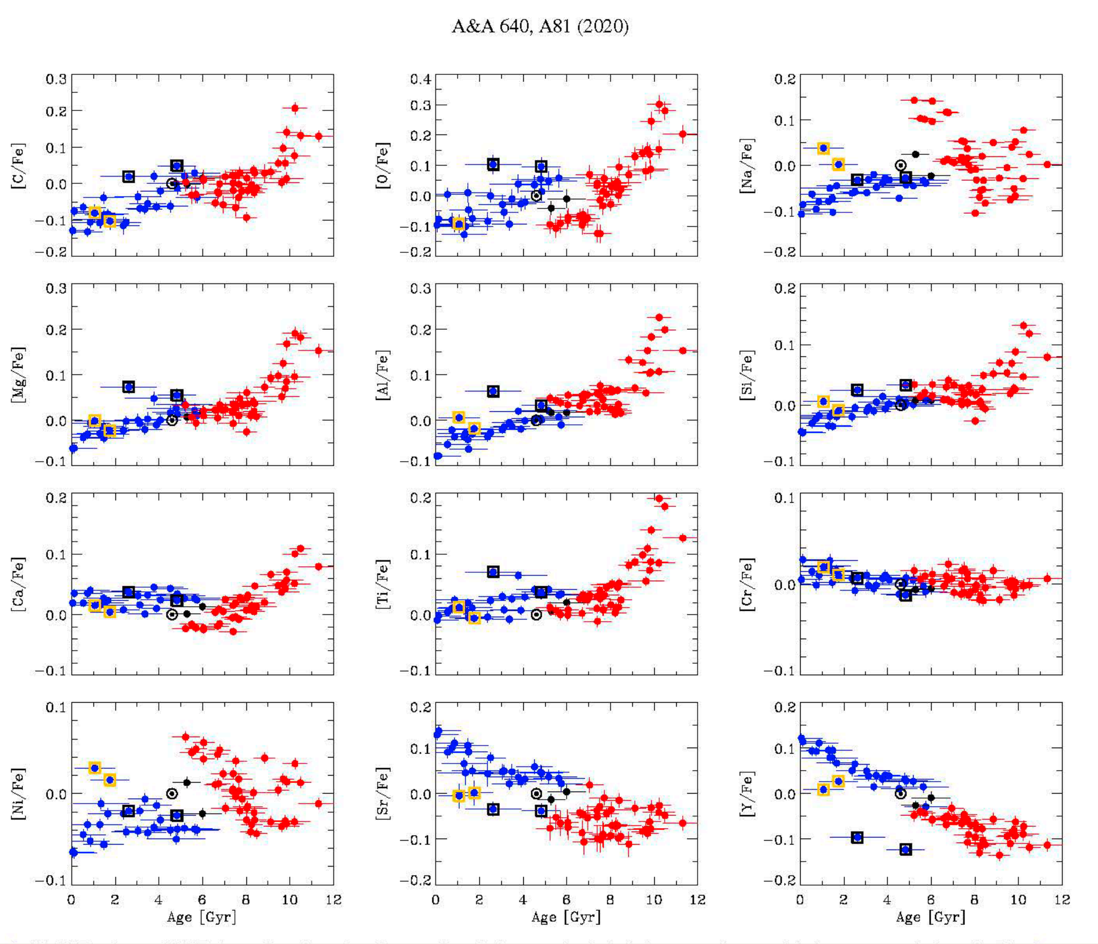

Nissen etal A&A 640 A81 2020

MNRAS 453, 1855–1866 (2015) doi:10.1093/mnras/

Carbon, nitrogen and α-element abundances determine the formation sequence of the Galactic thick and thin discs

T. Masseron★ and G. Gilmore

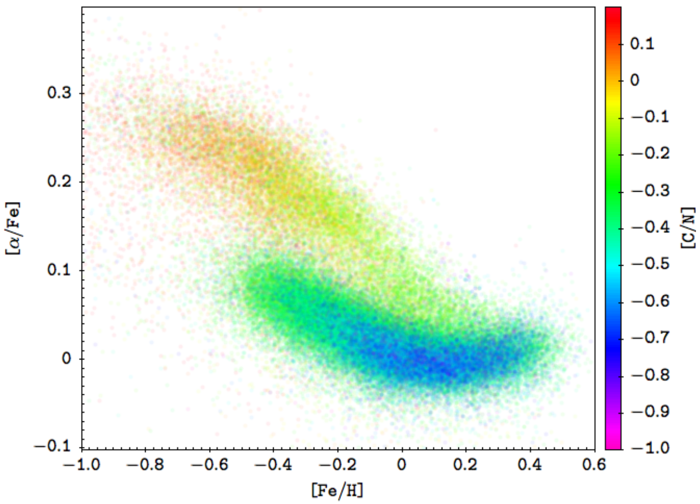

Fig. 11. [α/Fe] as a function of [Fe/H] for field stars in the APOGEE DR14 and a Gaia-ESO DR5 samples. The stars are colour-coded by [C/N].

Determine ages for RGB stars using dredge-up, which depends on stellar mass, hence age

The Gaia-ESO survey: Calibrating the relationship between Age and the [C/N] abundance ratio with open clusters★

G. Casali[1,2], L. Magrini[2], E. Tognelli[3], R. Jackson[4], R. D. Jeffries[4], N. Lagarde[5], G. Tautvaišienė[6], T. Masseron[7,8], S. Degl'Innocenti[3], P. G. Prada Moroni[3], G. Kordopatis[9], E. Pancino[2,10], S. Randich[2], S. Feltzing[11], C. Sahlholdt[11], L. Spina[12], E. Friel[13], N. Sanna[2], A. Bragaglia[14], A. Drazdauskas[6], Š. Mikolaitis[6], R. Minkevičiūtė[6], E. Stonkutė[6], Y. Chorniy[6], V. Bagdonas[6], F. Jimenez-Esteban[15], S. Martell[16,17], G. Gilmore[18], A. Vallenari[19], T. Bensby[11], S. E. Koposov[20], A. Korn[21], C. Worley[18], R. Smiljanic[22], M. Bergemann[23], G. Carraro[24], F. Damiani[25], E. Franciosini[2], A. Gonneau[18], A. Hourihane[18], J. Lewis[18], L. Morbidelli[2], G. Sacco[2], S. G. Sousa[26]

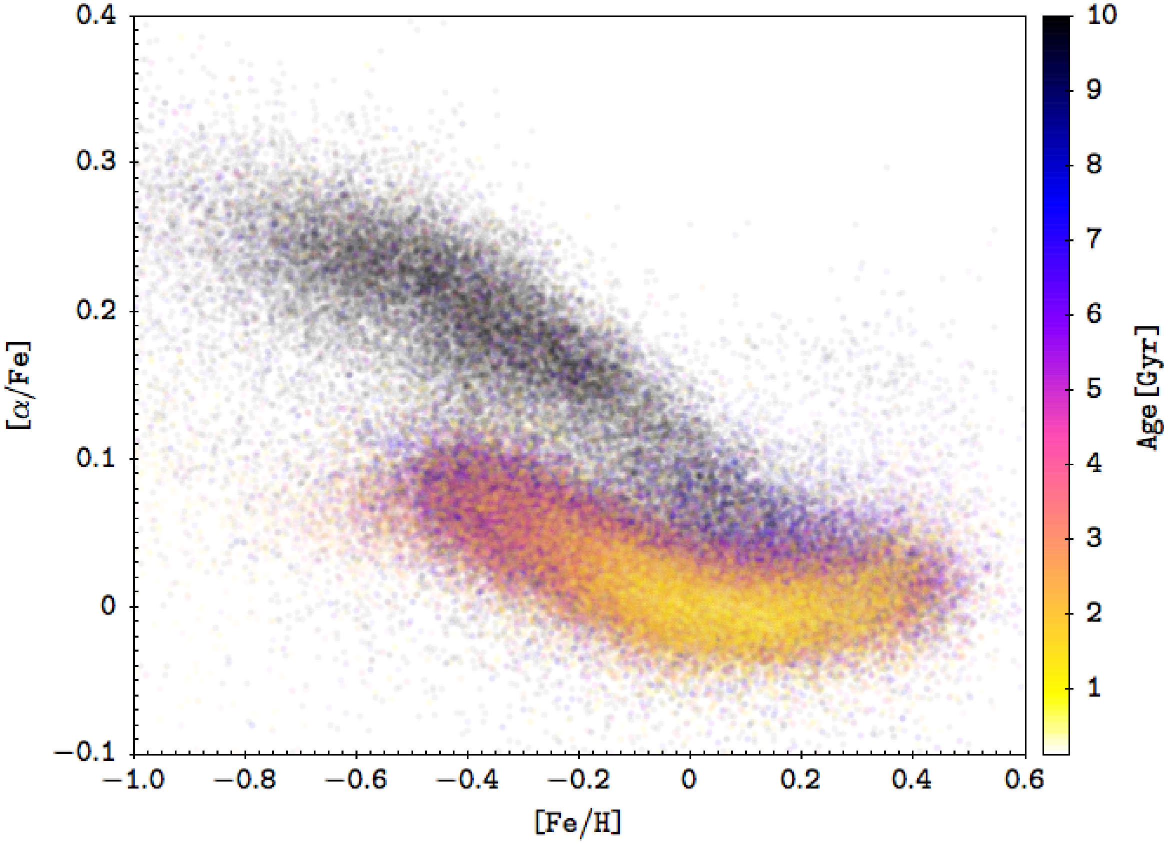

Fig. 12. [α/Fe] as a function of [Fe/H] for field stars in the APOGEE DR14 and a Gaia-ESO DR5 samples. The stars are colour-coded by ages.

The formation of disks: seeing the time line

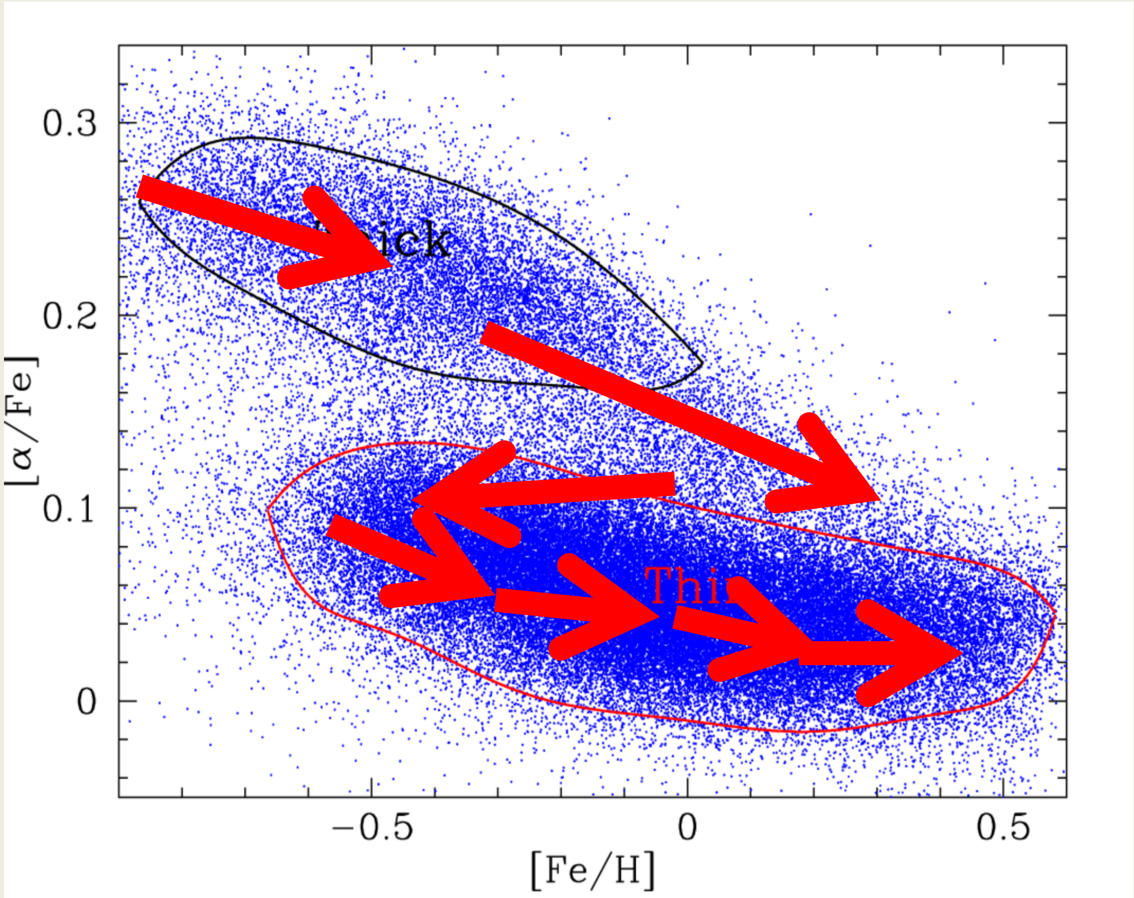

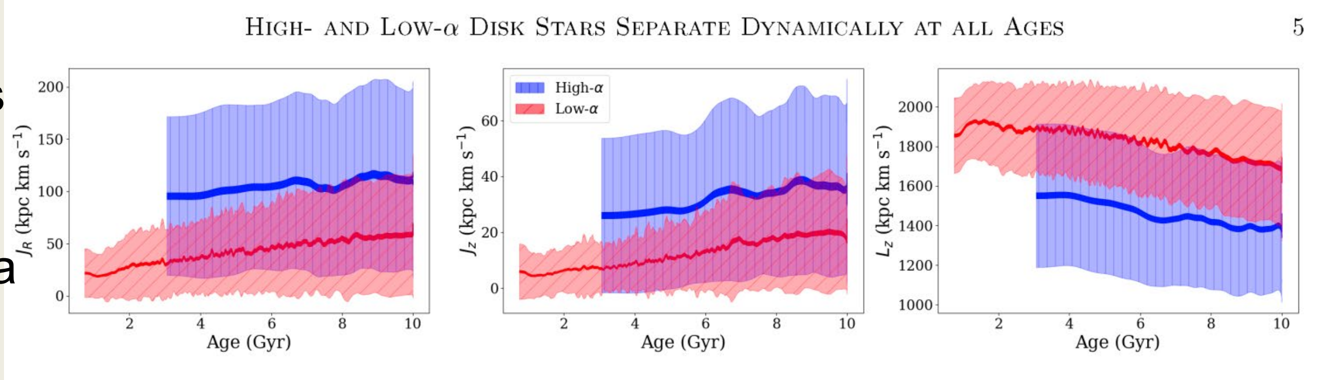

Gandhi+Ness
1903.04030

LAMOST data

DR2: halo x2

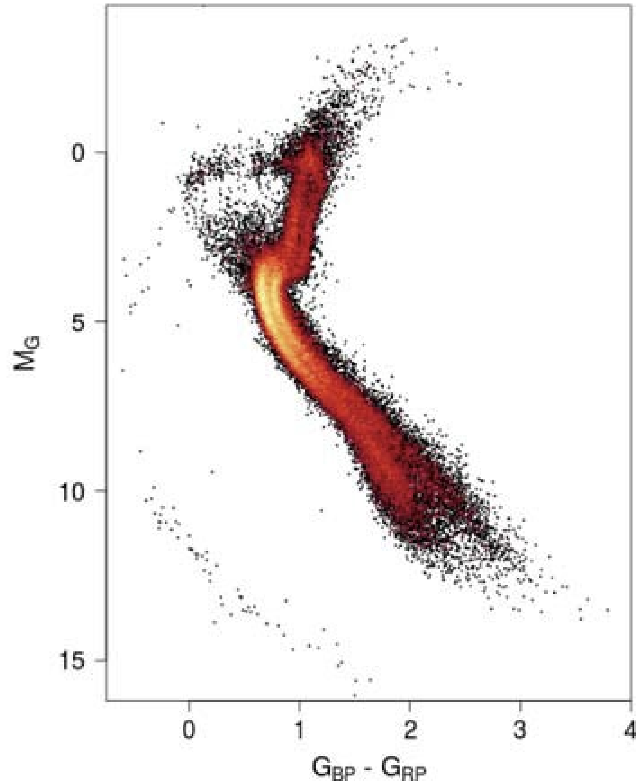

Halo stars on highly radial orbits
Kinematic evidence for the early (z~2) merger which puffed-up the thick disk

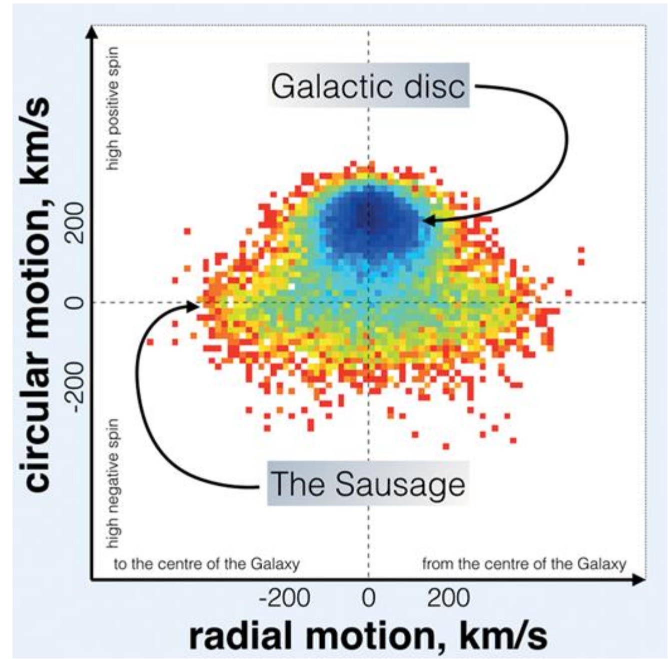

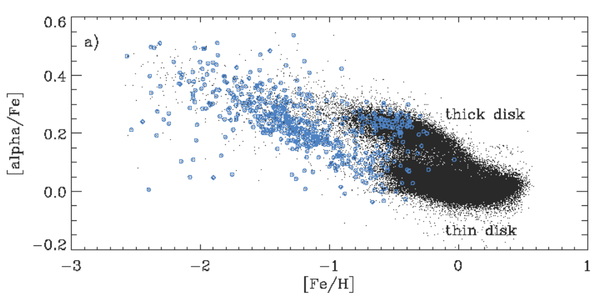

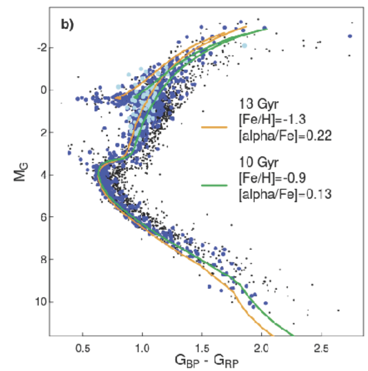

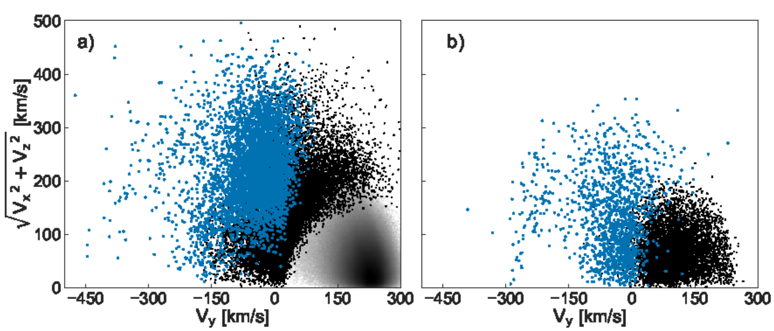

Belokurov etal; Helmi etal

Gaia's magic

The hidden giant: discovery of an enormous Galactic dwarf satellite in *Gaia* DR2

G. Torrealba,[1⋆] V. Belokurov,[2,3] S. E. Koposov,[4,2] T. S. Li,[5,6] M. G. Walker[4]
J. L. Sanders,[2] A. Geringer-Sameth,[7] D. B. Zucker,[8,9] K. Kuehn[10], N. W. Evans[2],
W. Dehnen[11,12]

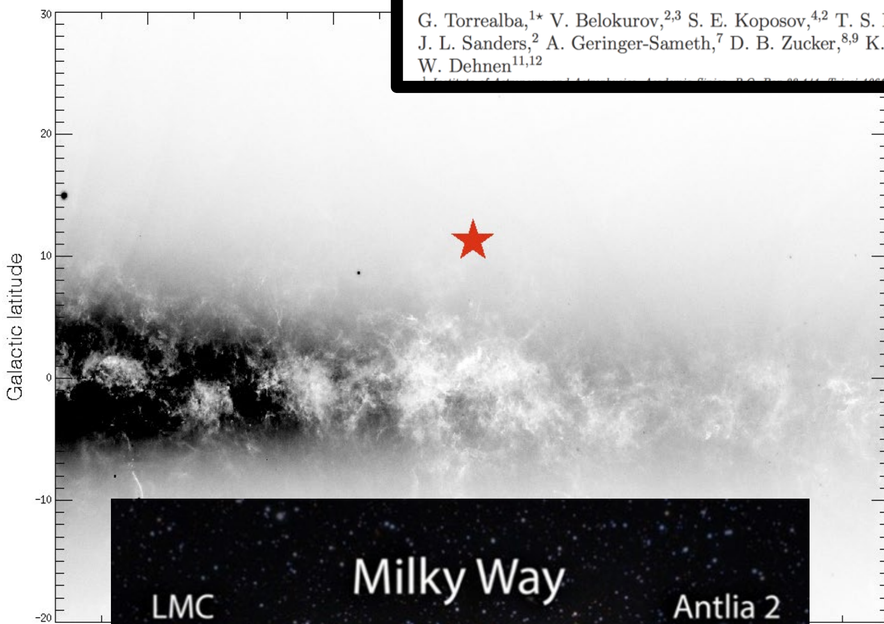

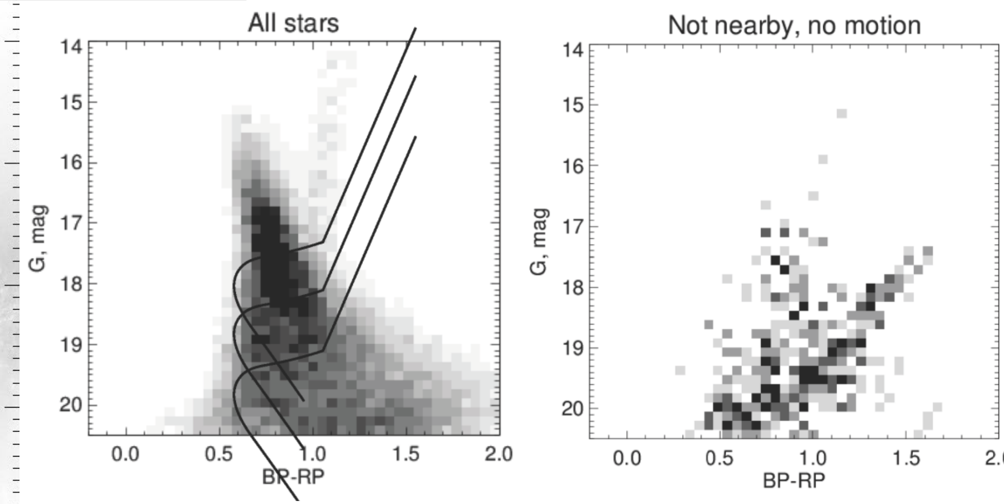

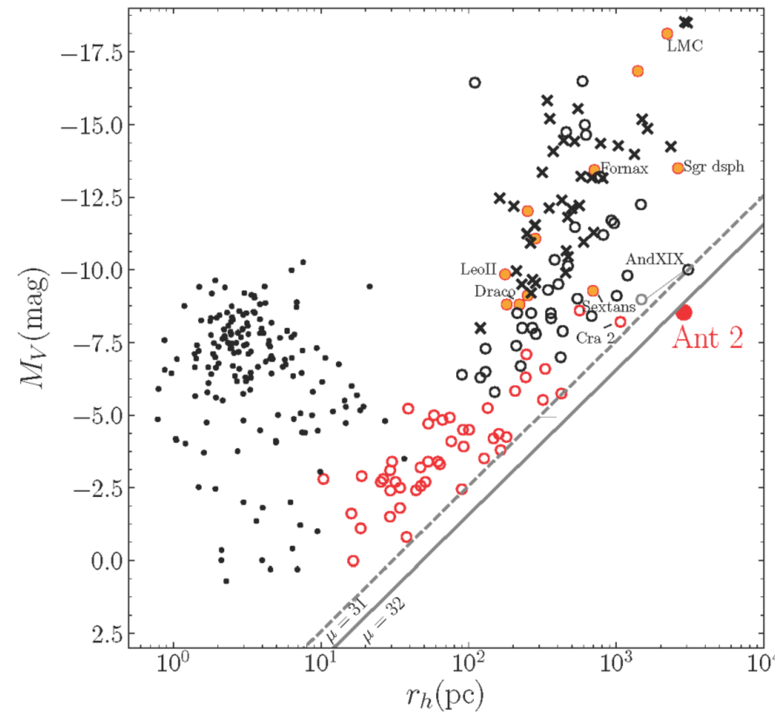

Antlia2 &LMC –
Same half-light radius
Total mass differ by 2 orders
Stellar masses differ by 4 orders

Quite inconsistent with theory

Field of Streams: SDSS stars vs distance

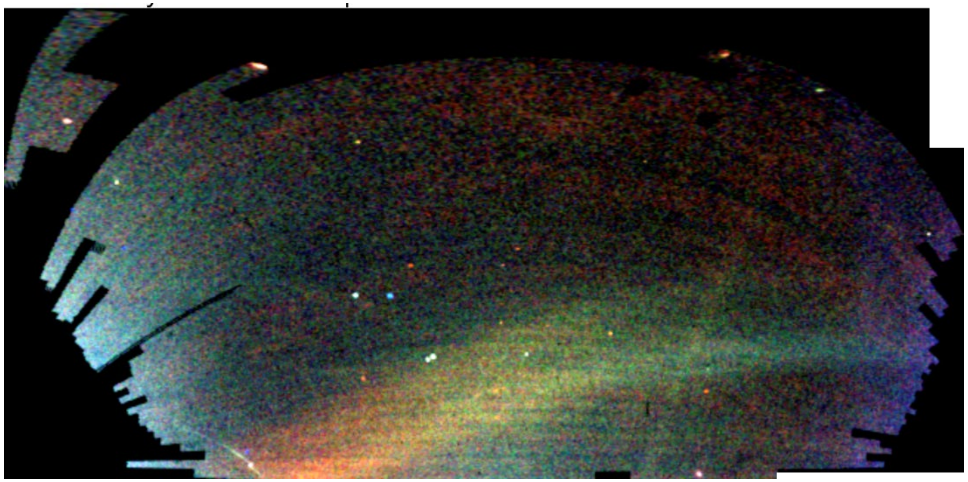

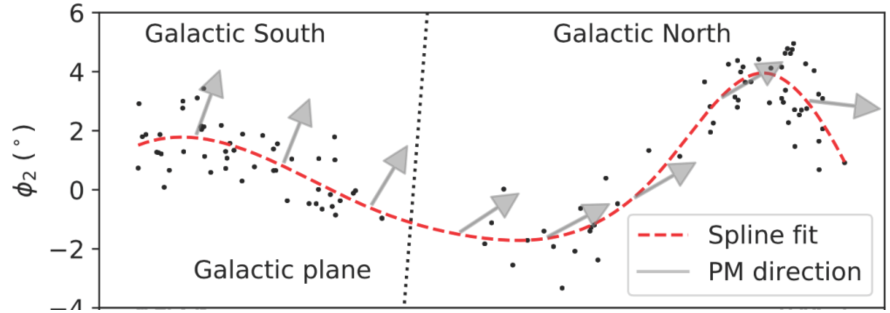

Modelling Gaia PMs in Orphan Stream gives total mass of LMC – First ever total galaxy mass

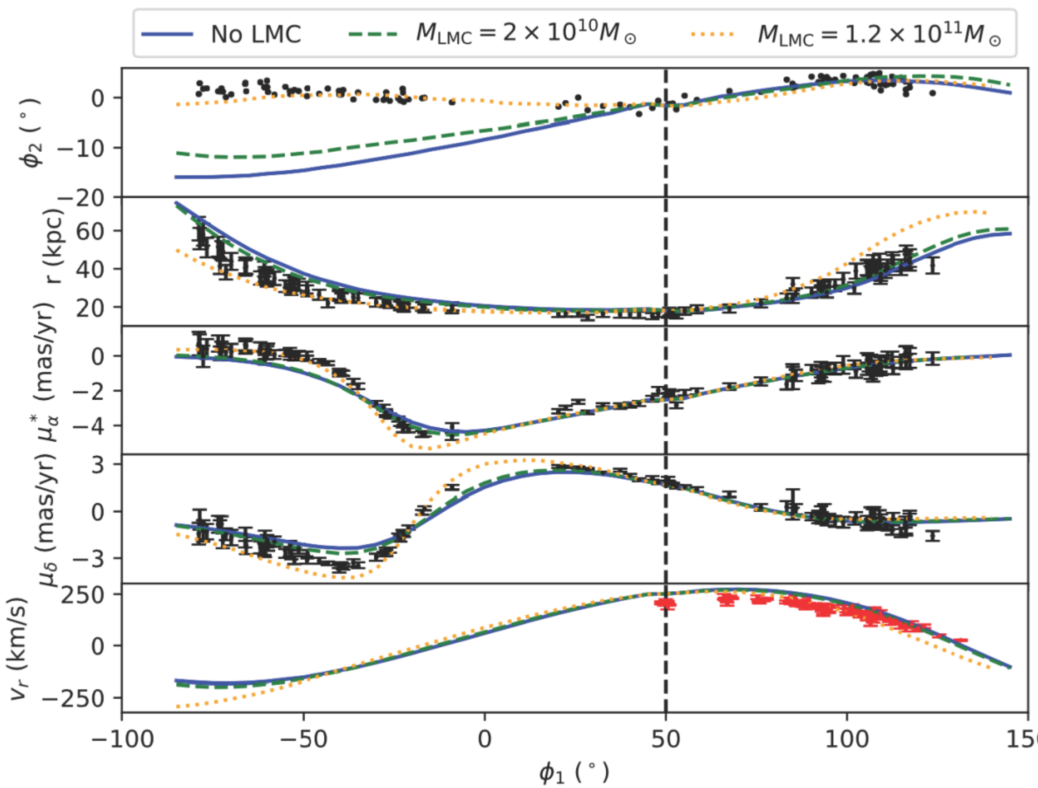

The total mass of the Large Magellanic Cloud from its perturbation on the Orphan stream

D. Erkal,[1*] V. Belokurov,[2,3] C. F. P. Laporte,[4] S. E. Koposov,[5,2] T. S. Li,[6,7] C. J. Grillmair,[8] N. Kallivayalil,[9] A. M. Price-Whelan,[10] N. W. Evans,[2] K. Hawkins,[11] D. Hendel,[12] C. Mateu,[13] J. F. Navarro,[14] A. del Pino,[15] C. T. Slater,[16] and S. T. Sohn[15]

(The OATs: Orphan Aspen Treasury Collaboration)

MilkyWay-Sgr-LMC orbits

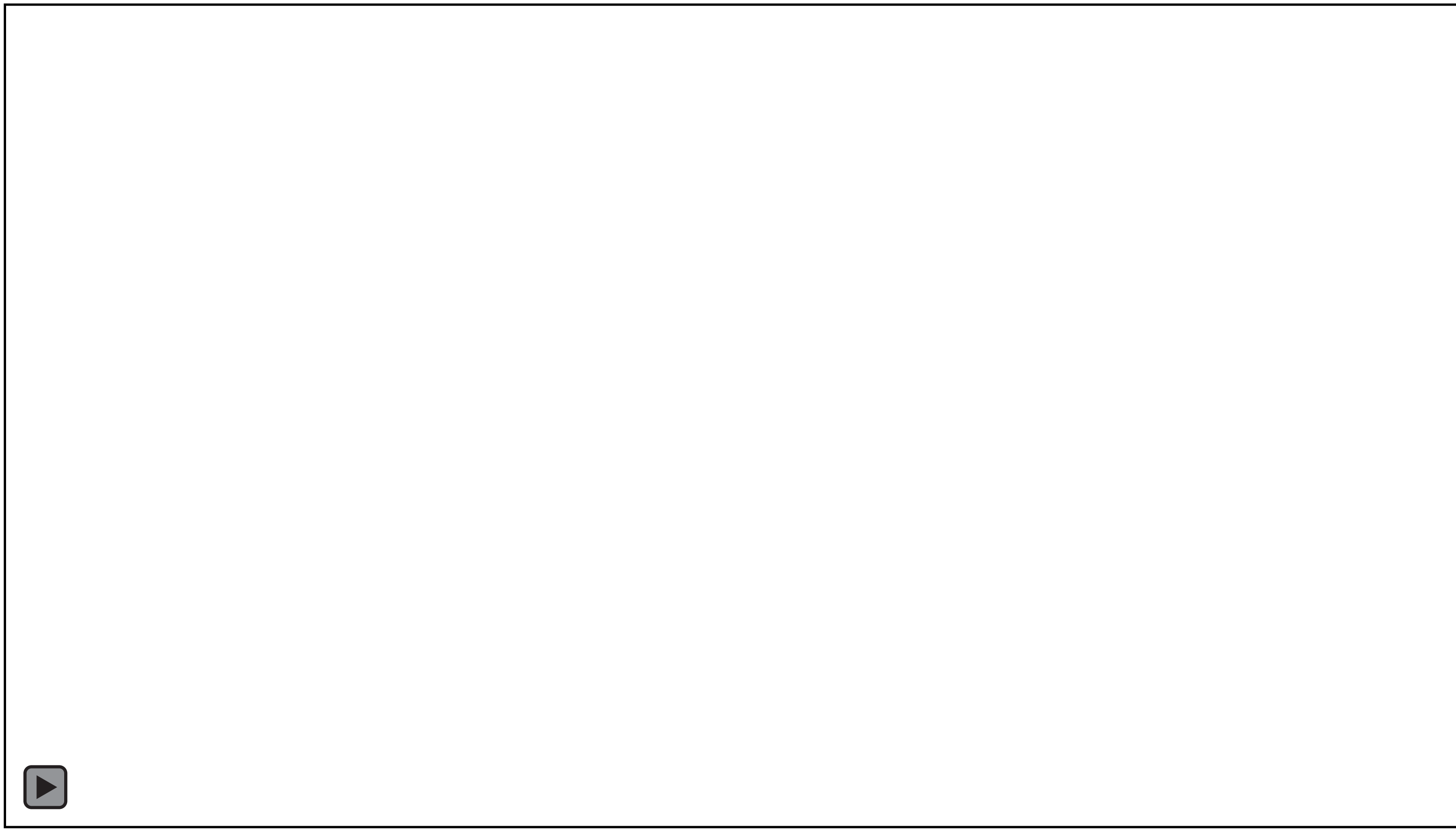

The astrometric GW sky

A passing GW imposes a – low amplitude! – quadrupole distortion on the sky

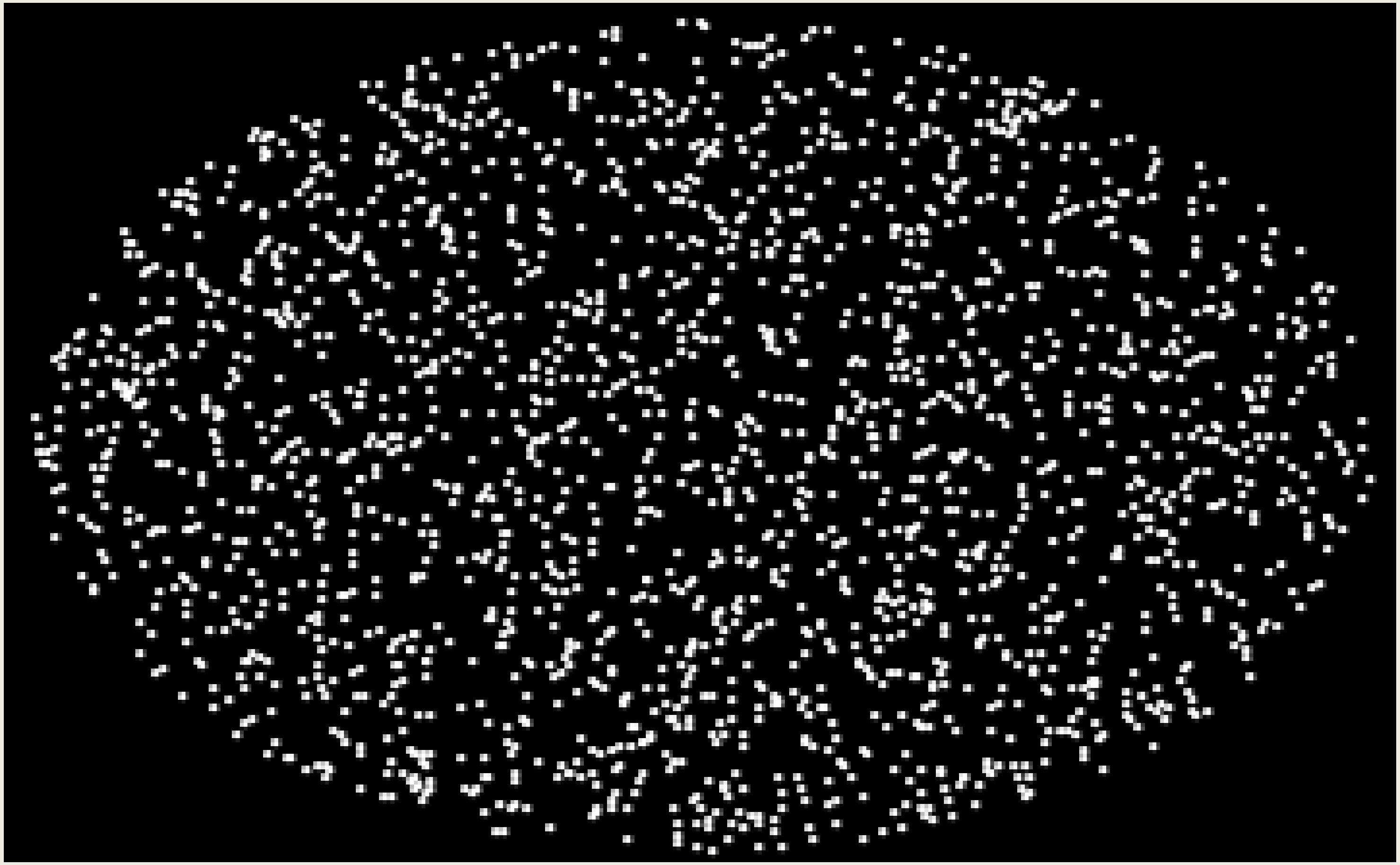

Simulation by Mihailovic, Moore, Gilmore, Lasenby

PHYSICAL REVIEW D 97, 124058 (2018)

Astrometric effects of gravitational wave backgrounds with non-Einsteinian polarizations

Deyan P. Mihaylov,[1,*] Christopher J. Moore,[2,3,†] Jonathan R. Gair,[4,‡]
Anthony Lasenby,[5,6,§] and Gerard Gilmore[1,∥]

PHYS. REV. D 97, 124058 (2018)

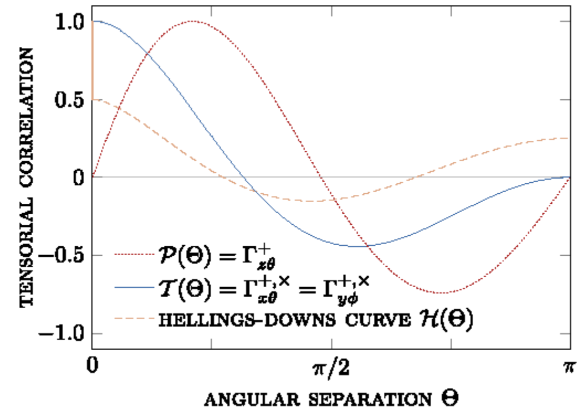

FIG. 5. The astrometric and redshift correlations as a function of angular separation on the sky in a background of tensorial, transverse-traceless GWs (i.e., + and ×). The well-known Hellings-Downs curve, $\mathcal{H}(\Theta)$, determines the redshift correlations and is shown here with the usual normalization $\lim_{\Theta\to 0} H(\Theta) = \frac{1}{2}$ due to the presence of the pulsar term in Eq. (17). The astrometric correlations are similarly determined by a single function, $\mathcal{T}(\Theta)$, which is shown with the normali-

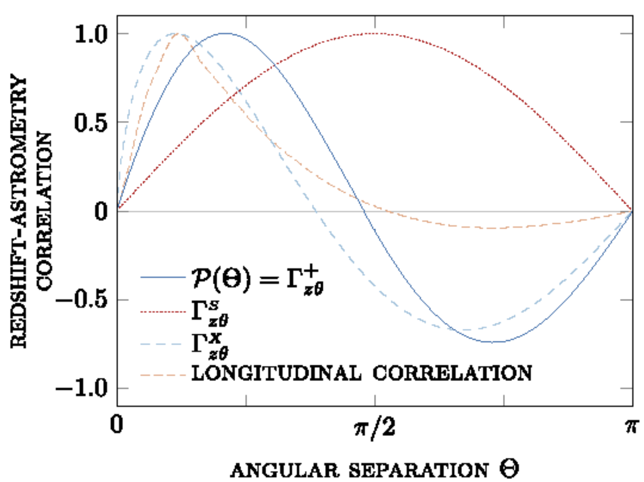

FIG. 12. The redshift-astrometric correlations as a function of angular separation on the sky, given by Eqs. (53), (55), and (56) for different polarizations. The numerical result for the scalar longitudinal correlation is plotted too (see Appendix F 1). All functions are normalized so that their maximum is unity.

A gravitational wave has 6 possible polarizations, though GR has two (+, X). Combined pulsar-astrometry analysis strengthens pure GR, and tests beyond GR

Gaia Statistics @ 07-June-2021

CURRENT DATE AND TIME	2021-06-07T16:09:47 (TCB)
MISSION STATUS	
Satellite distance from Earth (in km)	1,564,619
Number of days having passed since 25 July 2014	2509
Number of days in mission extension	692
OPERATIONS DATA (collected since 2014/07/25)	
Volume of science data collected (in GB)	93,501
Number of object transits through the focal plane	177,436,718,550
Number of astrometric CCD measurements	1,749,019,082,845
Number of photometric CCD measurements	352,491,043,206
Number of spectroscopic CCD measurements	34,476,063,279
Number of object transits through the RVS instrument	11,566,652,878

during this talk Gaia measured ≈3,000,000 objects

(…including 0.5M spectra, 6M photometry, 25M astrometry points)

Data taking until early 2025

Summary

- Gaia data are precise, accurate, getting better
- Calibration improving – will fix Cepheids
- Galaxy evolution mapped – dynamics and chemistry and star-ages probes
- Non-equilibrium limits disk DM study
- Outer streams/mergers probe DM better
- Lots more still to come


The people behind Gaia
The Gaia mission

Seeing stellar evolution!

A Gap in the Lower Main Sequence Revealed by *Gaia* Data Release 2

Wei-Chun Jao,[1] Todd J. Henry,[2] Douglas R. Gies,[3] and Nigel C. Hambly[4]

An explanation for the gap in the Gaia HRD for M-dwarfs

James MacDonald & John Gizis
Department of Physics and Astronomy, University of Delaware, Newark, DE 19716, USA

Abstract

We show that the recently discovered narrow gap in the Gaia Hertzsprung - Russell Diagram near $M_G = 10$ can be explained by standard stellar evolution models and results from a dip in the luminosity function associated with mixing of ^{3}He during merger of envelope and core convection zones that occurs for a narrow range of masses.

Key words: stars: evolution - stars: low-mass - (stars:) Hertzsprung–Russell and colour–magnitude diagrams, stars: luminosity function, mass function

Introduction

Based on measurements presented in Gaia Data Release 2 (Gaia Collaboration et al. 2016, 2018), Jao et al. (2018) have reported their discovery of a narrow gap in the main sequence on the Hertzsprung - Russell Diagram (HRD) near $M_G = 10$. The gap is near spectral type M3V where M dwarf stars are thought to transition from partially to fully convective, and Jao et al. propose that the gap is linked to the onset of full convection in M dwarfs.

Here we show that the gap is a feature of existing models and is due to a dip in the luminosity function associated with mixing of ^{3}He during merger of envelope and core convection zones. The narrowness of the gap is a result of the small mass range over which this merger can occur.

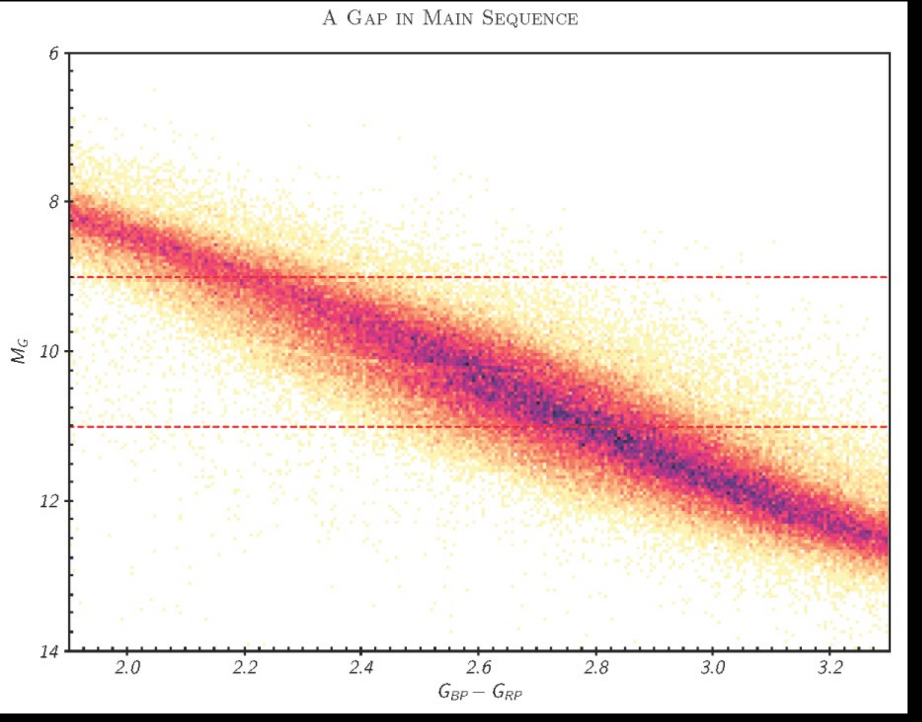

Extended Main Sequence Turnoffs in Open Clusters as Seen by Gaia: I. NGC 2818 and the Role of Stellar Rotation

N. Bastian[1], S. Kamann[1], I. Cabrera-Ziri[2]★ , C. Georgy[3], S. Ekström[3], C. Charbonnel[3,4], M. de Juan Ovelar[1], and C. Usher[1]

[1]Astrophysics Research Institute, Liverpool John Moores University, 146 Brownlow Hill, Liverpool L3 5RF, UK

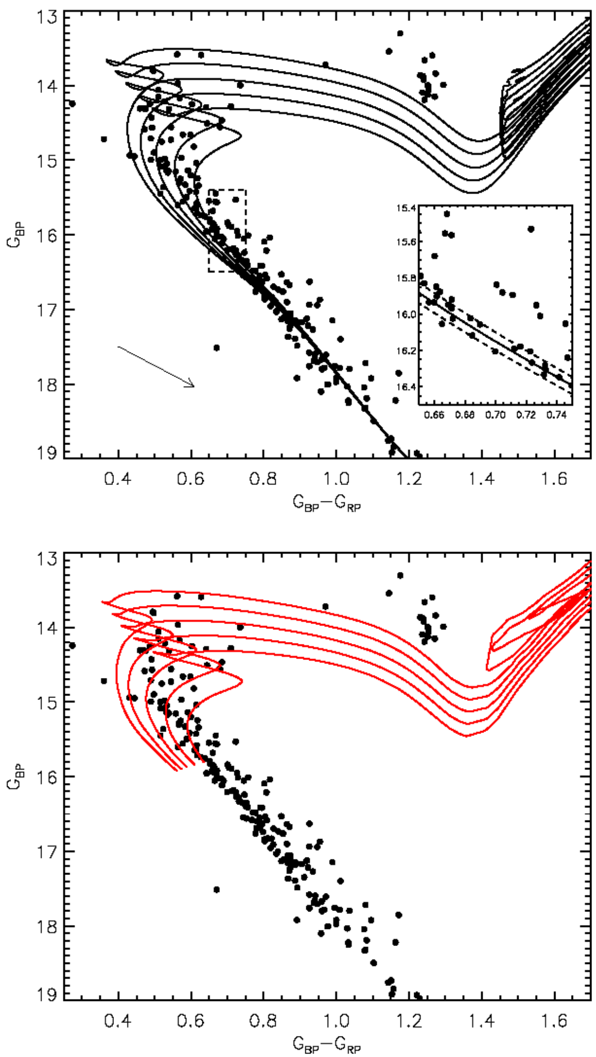

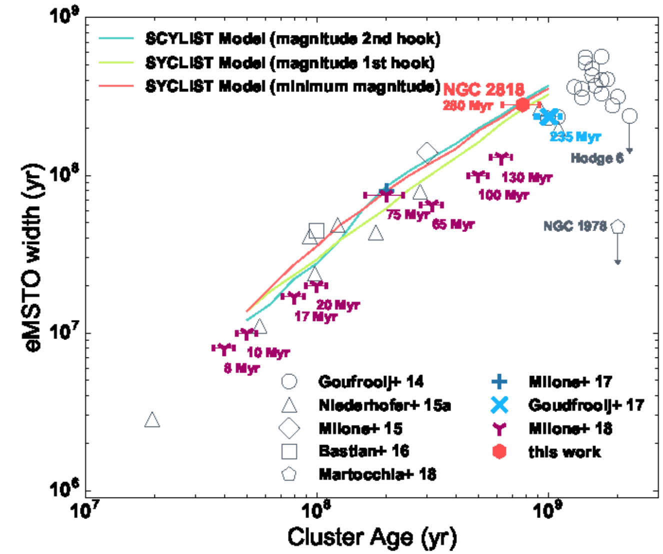

Figure 4. The relation between cluster age and inferred age spread for a sample of clusters from the literature as well as that found for NGC 2818 (see Niederhofer et al. 2015 for the original plot and a description of the models). We have added additional clusters from the literature in the past 3 years (see text). NGC 2818 follows the trend found for other cluster samples. The horizontal 'error bars' for the Goudfrooij et al. (2017) and Milone et al. (2018) samples show, assuming the inferred age spreads are real, when star formation began and terminated within each cluster. Solid lines show the expectations for rotating stellar models (Niederhofer et al. 2015).

4.2 The Origin of the Extended Main Sequence Phenomenon

The discovery of an eMSTO in a low mass (~ 2400 M$_\odot$), intermediate age (800 – 900 Myr) Galactic open cluster shows that the eMSTO phenomenon is not limited to high mass clusters, nor the special conditions of the LMC/SMC. Combining the clean CMD made possible from Gaia proper motions and parallaxes, with medium resolution

How young stars accumulate their mass. Gaia17bpi - 25th known FU Orionis star. First example caught in outburst in optical and IR

The new study shows, with the most detail yet, how material moves from the midrange of a disk, around 1 AU from the star, to the star itself.
As the material started to accumulate in the disk, it warmed up, giving off infrared light. Then, as this material fell onto the star, it heated up even more, giving off visible light, which is what Gaia detected.

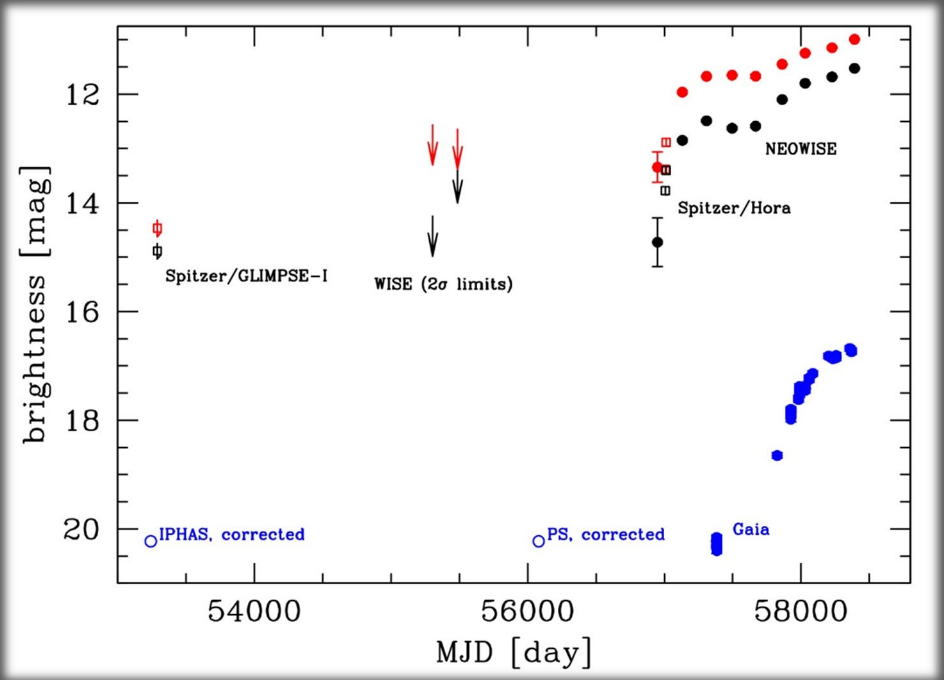

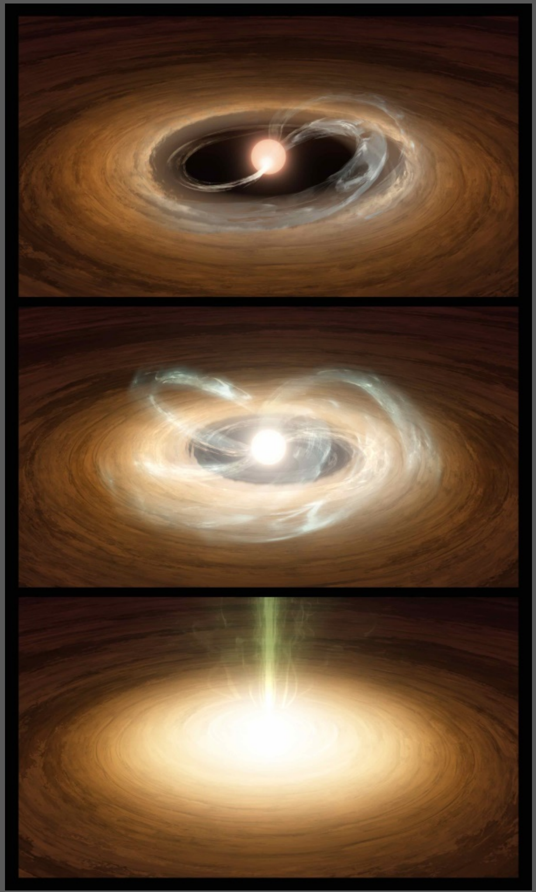

The *Gaia*-ESO Survey: Asymmetric expansion of the Lagoon Nebula cluster NGC 6530 from GES and *Gaia* DR2

Nicholas J. Wright[1], R.D. Jeffries[1], R.J. Jackson[1], A. Bayo[2,3], R. Bonito[4], F. Damiani[4], V. Kalari[5], A.C. Lanzafame[6], E. Pancino[7,8], R.J. Parker[9,⋆], L. Prisinzano[4], S. Randich[7], J.S. Vink[10], E.J. Alfaro[11], M. Bergemann[12], E. Franciosini[7], G. Gilmore[13], A. Gonneau[13], A. Hourihane[13], P. Jofré[14], S.E. Koposov[13], J. Lewis[13], L. Magrini[7], G. Micela[4], L. Morbidelli[7], G.G. Sacco[7], C.C. Worley[13] and S. Zaggia[15].

See star clusters dissolve in the Galactic tide

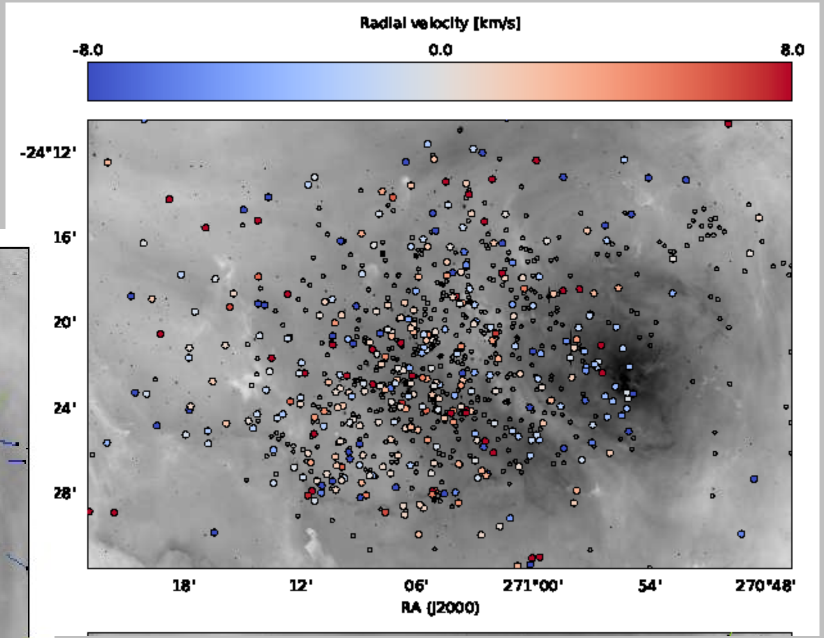

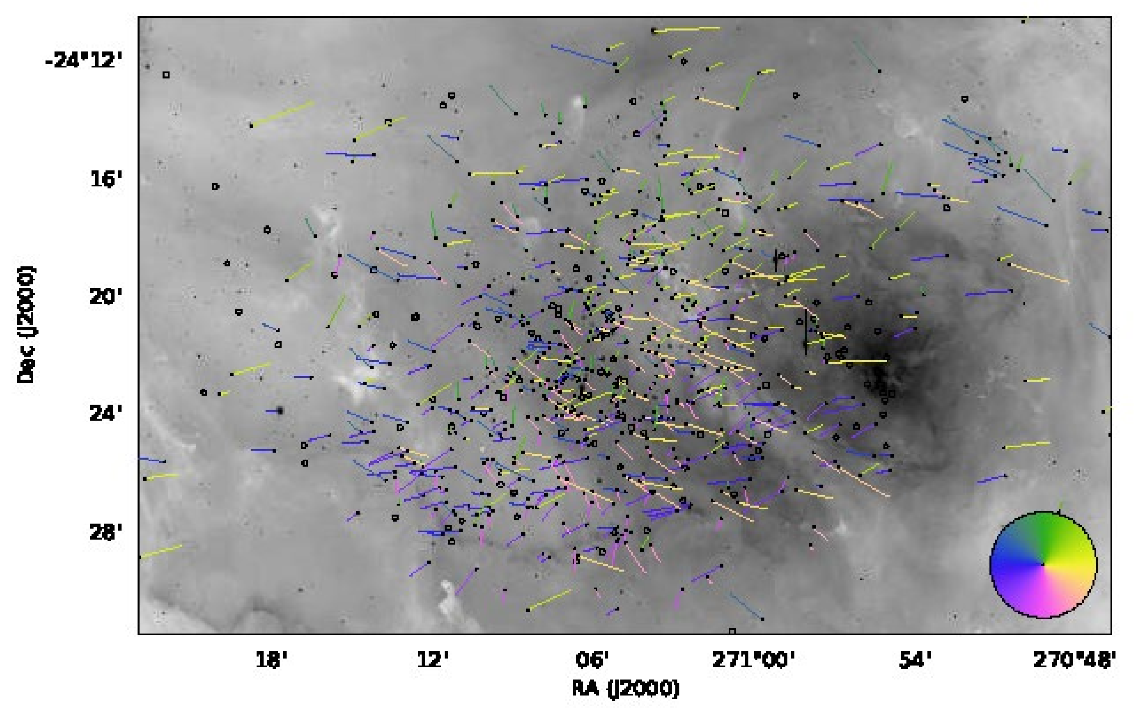

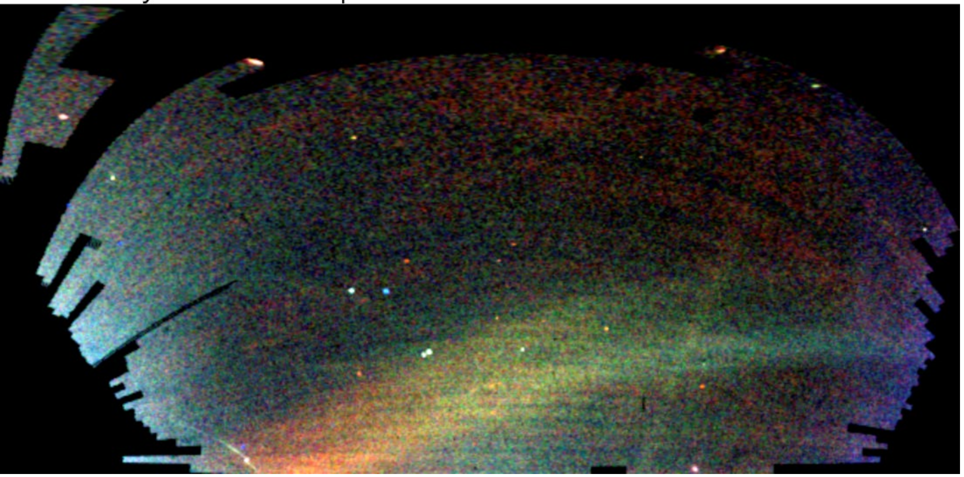

Modelling Gaia PMs in Sgr Stream shows 3-galaxy dynamical history

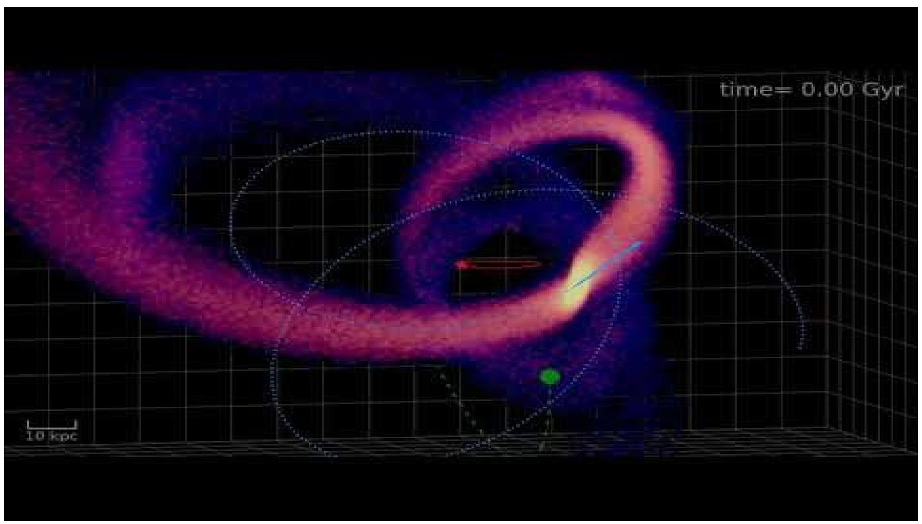

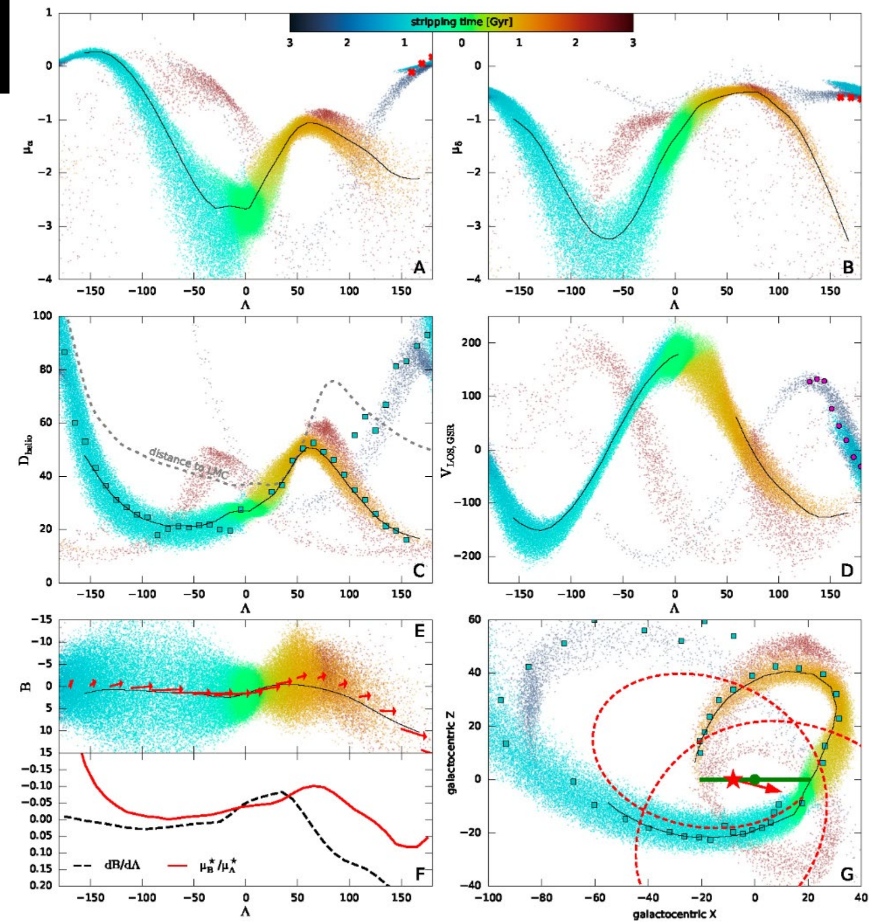

Vasiliev, Belokurov, Erkal arXiv:2009.10726